

Electronic Supporting Information

A Copper(II) Metal – Organic Hydrogel as Multifunctional Precatalyst for CuAAC Reaction and Chemical Fixation of CO₂ Under Solvent Free Condition

Chandan Kumar Karan, Mohan Chandra Sau and Manish Bhattacharjee*

[#]Department of Chemistry, Indian Institute of Technology Kharagpur,

Kharagpur- 721302, India.

*E-mail: mxh@iitkgp.ac.in

Table of Contents

1. Experimental Section	S3-S5
2. Figure S1: Formation of Cu-MOG	S6
3. Figure S2: Thixotropic & chemoresponsive behaviour	S6
4. Figure S3: Rheology plot	S7
5. Figure S4: TGA of Cu-MOG	S7
6. Figure S5: N ₂ and CO ₂ adsorption isotherm of Cu-MOG	S8
7. Figure S6: PXRD	S8
8. Figure S7: MALDI-TOF spectrum	S9
9. Figure S8: Index of peaks of MALDI-TOF spectrum	S9
10. Figure S9: XPS spectrum of Cu-MOG	S10
11. Figure S10: FESEM elemental analysis of Cu-MOG	S10
12. Table S1: Comparison table for CuAAC reaction	S11
13. Table S2: Comparison table for gas adsorption by MOGs	S12

14.Characterization data of products	S13-S16
15.NMR Spectra	S17-S29
16.HRMS Spectra	S30-S31
17.Yield calculation of cyclic carbonates from ¹H-NMR	S32-S43
18.References	S44

Experimental Section

General Information

All the chemicals, iminodiacetic acid was bought from Merck, 2,4-di-tert-butylphenol was bought from Sigma-Aldrich and copper chloride, alkynes were commercially available and used as received. Azides were synthesized according to the standard procedure from literature. Propylene oxide, 1,2-epoxyhexane were bought from Sigma-Aldrich and styrene oxide were bought from Merck. Analytical reagent grade solvents were used as received without further distillation.

Synthesis of Cu-MOG

In a typical gel formation experiment, 8 mg (0.04 mmol/mL) of ligand (Na_2HL) was dissolved in 0.5 ml of water and placed in six different glass vials, and 0.2–1.0 equiv of metal salt (CuCl_2) with respect to the ligand concentration was also dissolved in water and placed in six different glass vials separately. Finally, the aqueous solution of metal salt added to the aqueous solution of Na_2HL such that the total volume of the solvent in each vial is 1 mL. Then the formation of gel was confirmed by glass vial inversion method after two minutes at room temperature in 1:1 metal and ligand ratio.

Field Emission Scanning Electron Microscope (FESEM)

The morphology of the Cu-MOG was characterized using a field emission scanning electron microscope (ZEISS EVO 60 with oxford EDS detector) operating at 5 KV. Sample was prepared by dropping the dilute solution of the Cu-MOG on the thin aluminum sheets and then dried in air. A thin layer of Au was coated on the sample to minimize sample charging before the experiment.

Atomic Force Microscope (AFM)

The aggregation of the Cu-MOG was characterized by atomic force microscopy (Agilent 5500) in tapping mode. AFM sample was prepared by dropping the very dilute solution of Cu-MOG on a small piece of the glass slide and allowed to dry overnight before imaging.

Transmission Electron Microscopy (TEM)

The gel sample was characterized by an analytical TEM (FEI. TECNAIG220S-TWIN) instrument operating at 200 KV. Sample was prepared by dropping the much dilute solution of the Cu-MOG on the carbon-coated copper grid and the sample was allowed to dry for overnight before experiment.

Optical Microscopy (OM)

The gel sample was characterized by an optical image analyzer (Leica DMLM) instrument. The sample was prepared by dropping the very dilute solution of the Cu-MOG on the glass slide.

Rheological Measurements

The rheological experiments were carried out on an MCR 102 (Anton paar) modular compact rheometer with the 25 mm diameter parallel plate having a constant tool gap of 0.5 mm. The stress amplitude sweep experiment was carried out at a constant angular frequency of 1 rad sec^{-1} at 298K. The frequency sweep measurement was carried out in the linear viscoelastic range at a constant stress.

Gas Sorption Study

The gas sorption experiment was carried out on the dried xerogel of Cu-MOG using a Micromeritics 3flex gas adsorption analyzer in a 6 mm sample holder at 77 K for N_2 and 273 K for CO_2 . Before the sorption experiment, the sample was employed for degassing at 100°C for 8 h.

MALDI-TOF

The MALDI-TOF spectrum of the Cu-MOG was taken using 2,5-dihydroxybenzoic acid as the matrix in the Bruker Daltonics, model: Ultraflextreme instrument.

General Procedure for the CuAAC Reaction

To a mixture of the benzylazide (**1a**, 133 mg, 1.0mmol) and phenylacetylene (**2a**, 102 mg, 1.0 mmol) in a vial the Cu-MOG catalyst (3.4 mg $\text{CuCl}_2 \cdot 2\text{H}_2\text{O}$ and 7.9 mg ligand, Na_2HL with 0.2 mL H_2O i.e 2 mol % copper complex calculated from MALDI-TOF spectrum) was added. The

mixture was stirred at 50 °C for the time given in the Tables (see text). After completion of the reaction, ethyl acetate (2 mL \times 2 times) was added and the mixture was centrifuged to recover the catalyst. The organic layer was concentrated and the crude product was purified by column chromatography. Before reuse, the recovered catalyst was washed with ethyl acetate (2 mL \times 3 times) and heated at 80 °C for 1 h.

General Procedure for the cycloaddition of CO₂ to epoxides

In a typical reaction, cycloaddition of the epoxide (10 mmol) was carried out with carbon dioxide purged at 1 bar in presence of tetrabutylammonium bromide (TBAB, 10 mol%) as a cocatalyst at room temperature under solvent free condition; while the xerogel as the catalyst was used 11.3 mg (0.2 mol % based on the Cu-MOG complex) for 48 hours. The yields of the products were calculated based on the ¹H NMR analysis.

To reuse the Cu-MOG, at first the reaction mixture was centrifuged to recover the catalyst. Then the clear solution was decanted and the epoxide (1,2-epoxy hexane) and TBAB was added. Then the reaction was done under same condition as previously described.

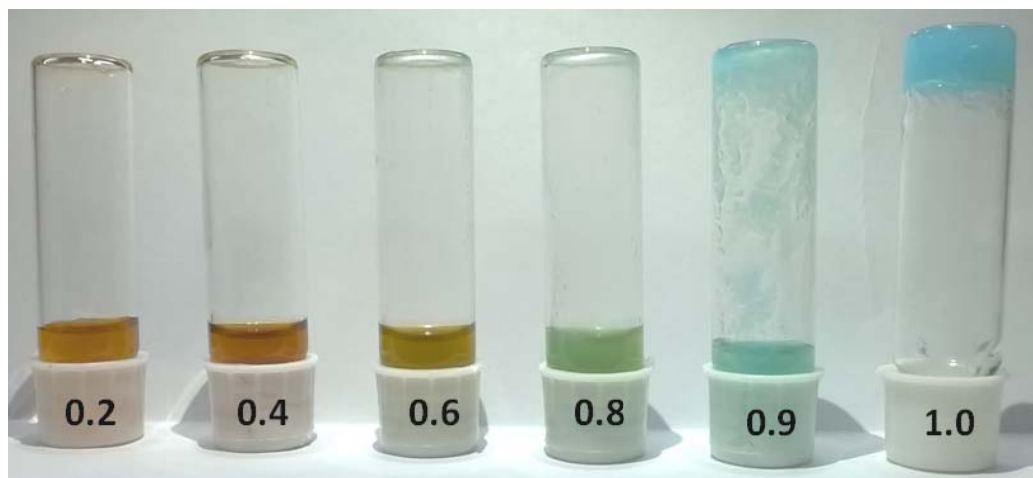


Figure S1. Image of inverted vials of Cu-MOG formation. Numbers on the cap indicates the equivalent amount of CuCl_2 with respect to ligand, Na_2HL present in the respective vial

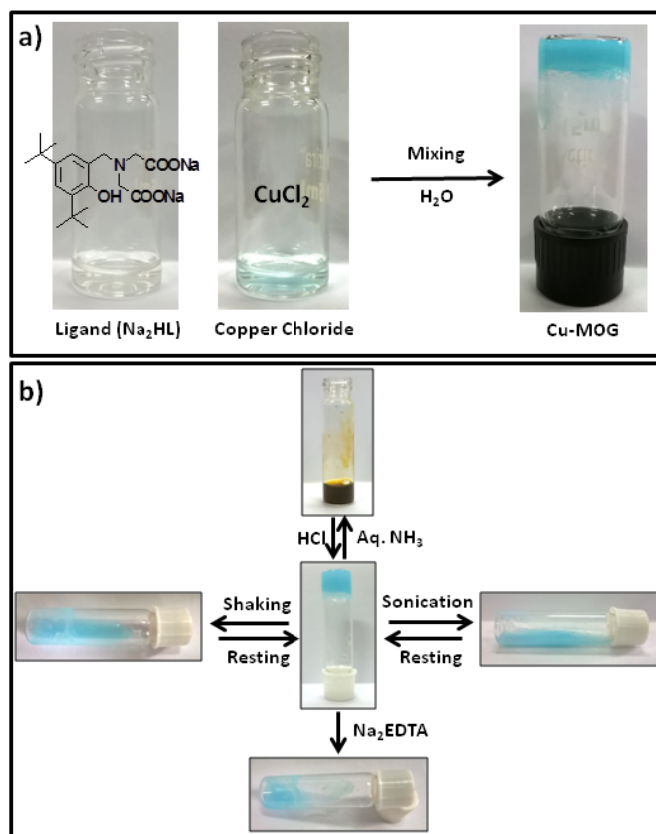


Figure S2. Formation (a) and multi-stimuli responsive nature (b) of metalhydrogel Cu-MOG

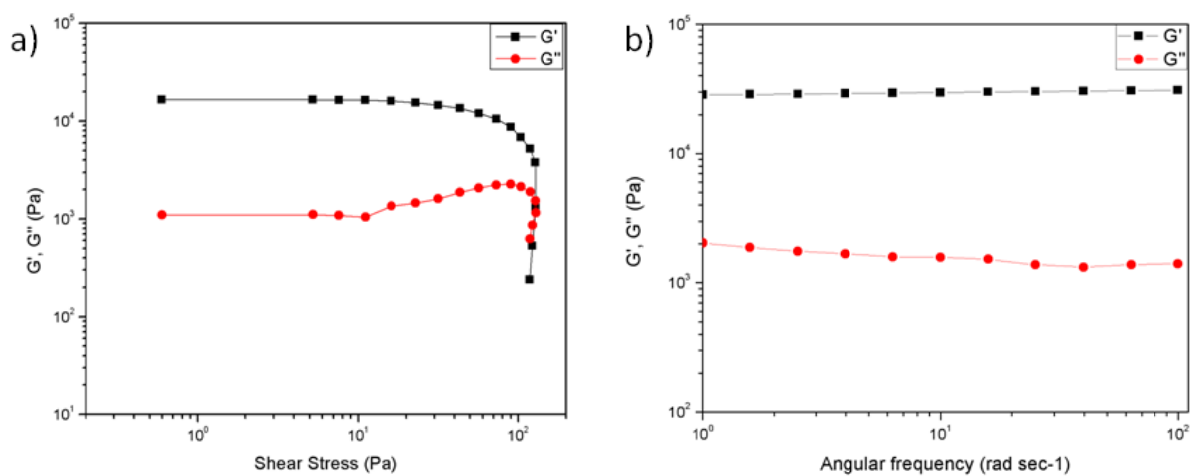


Figure S3. Plot of storage modulus (G') and loss modulus (G'') with (a) shear stress at 1 rad sec^{-1} and with (b) frequency at 0.01% strain for Cu-MOG

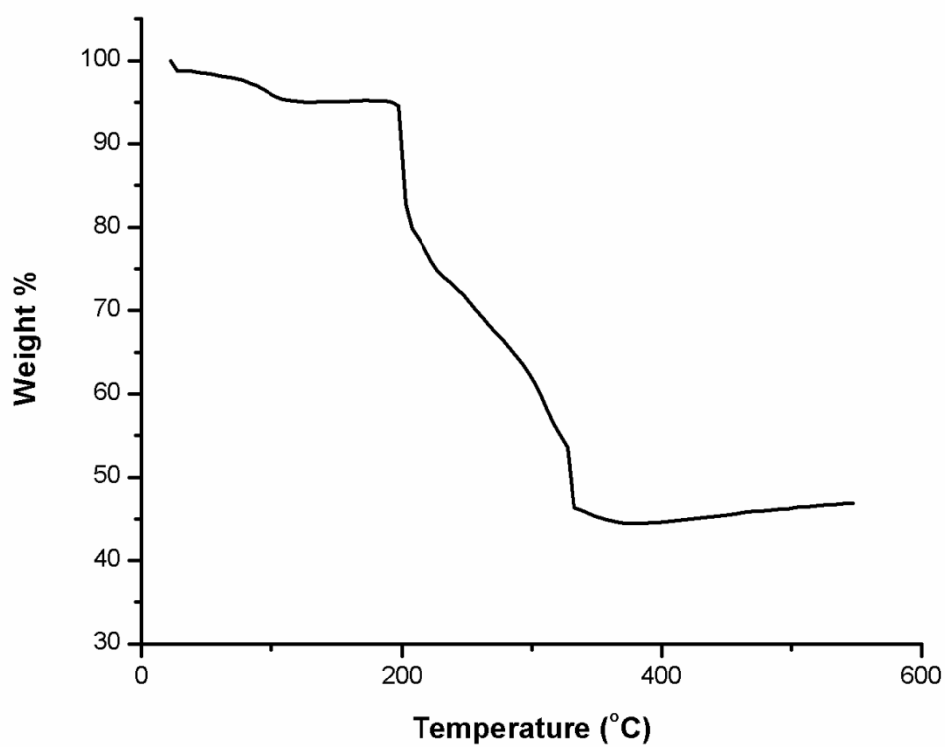


Figure S4. TGA curve of Cu-MOG

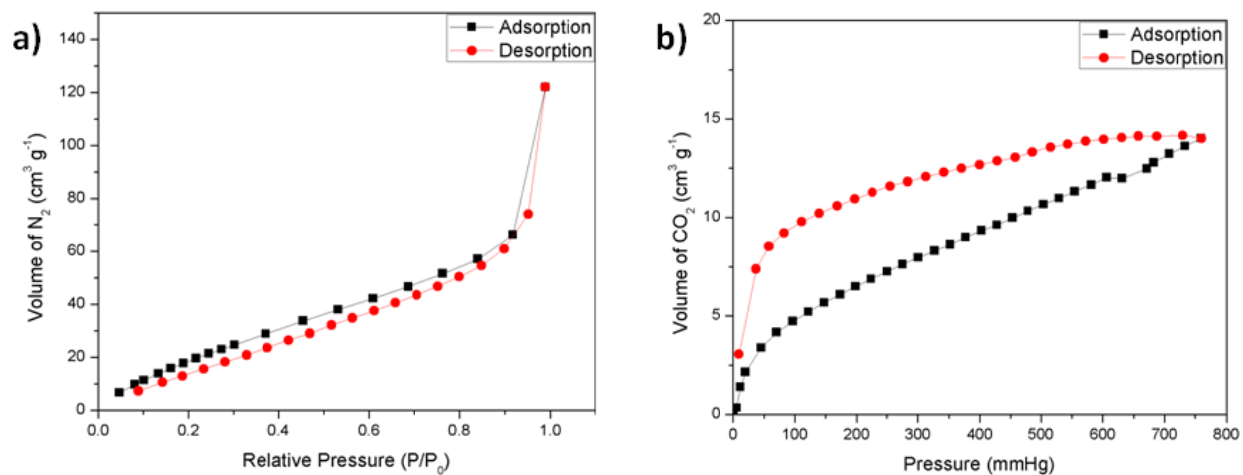


Figure S5. N_2 (a, at 77 K) and CO_2 (b, at 273 K) adsorption isotherm of Cu-MOG

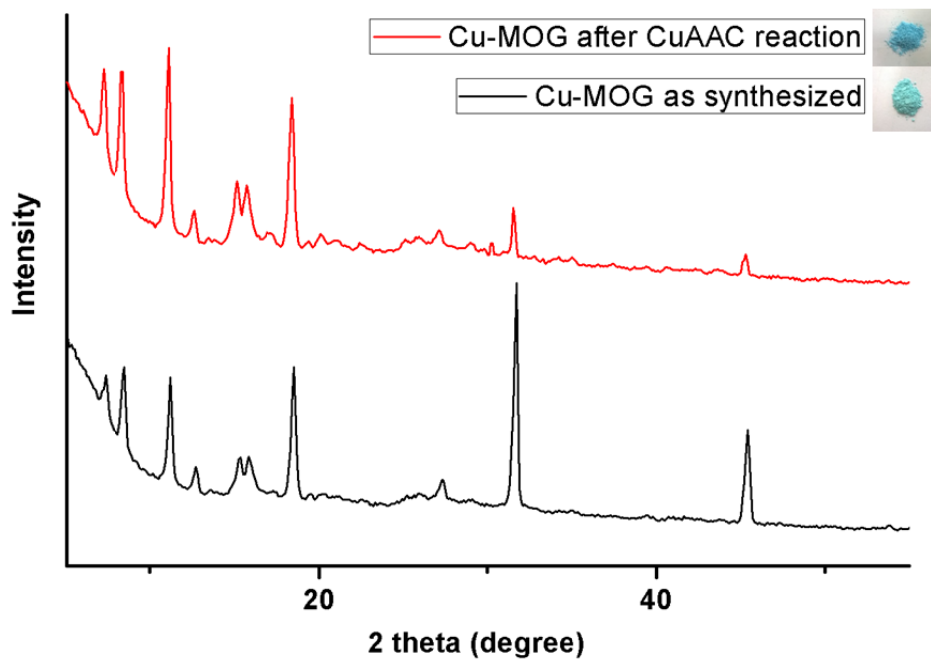


Figure S6. PXRD of as-synthesized Cu-MOG and Cu-MOG after catalytic reaction and the inset images of Cu-MOG are before (down) and after (up) catalytic reaction

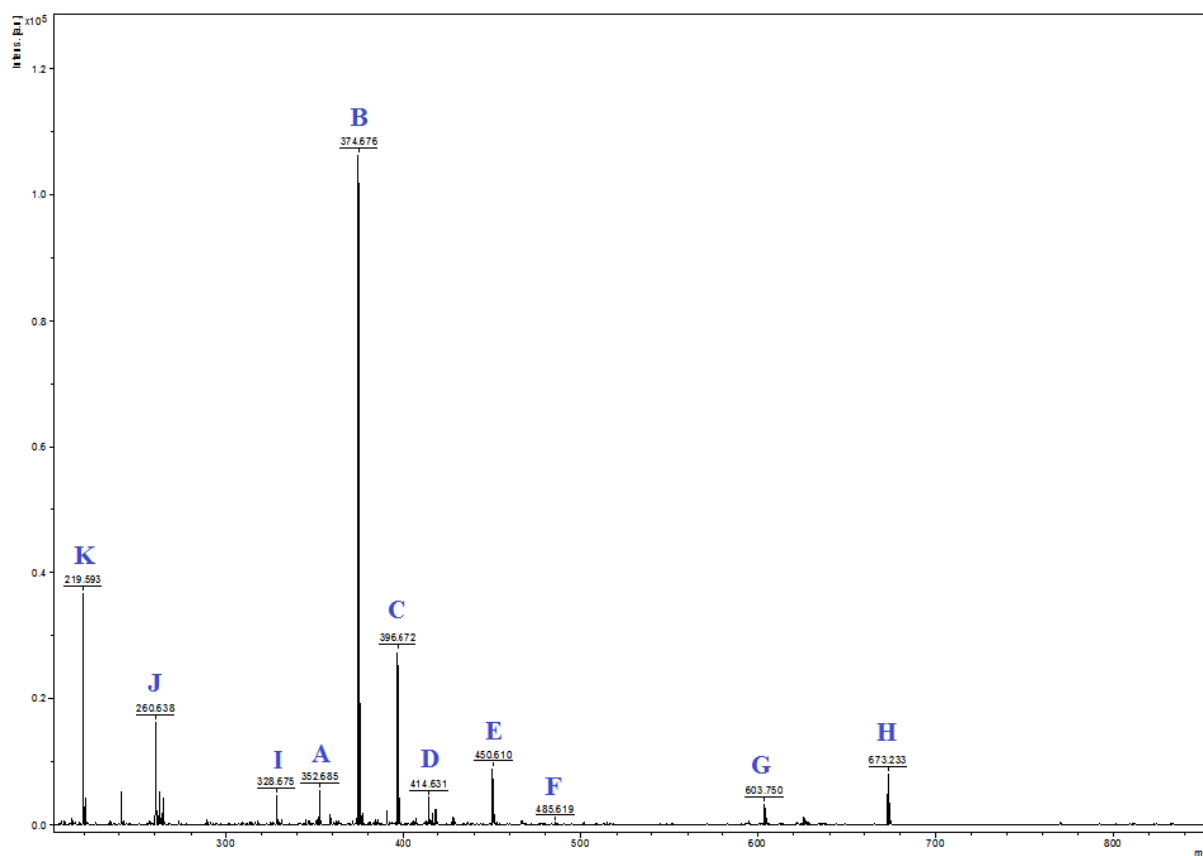


Figure S7. MALDI-TOF spectrum of the Cu-MOG in DHB matrix

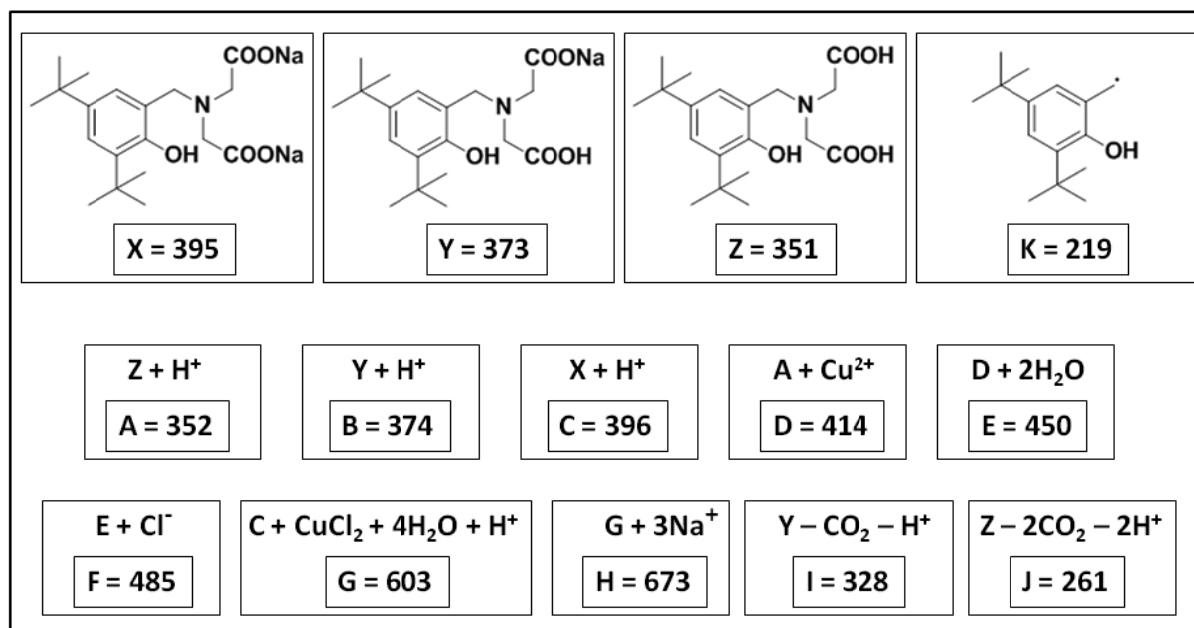


Figure S8. Index of peaks appearing in the MALDI-TOF spectrum

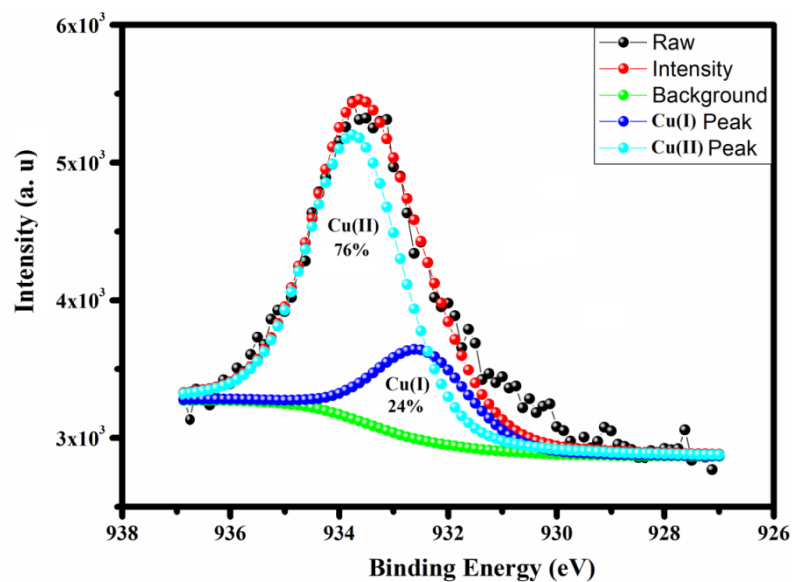


Figure S9. XPS spectrum of Cu-MOG

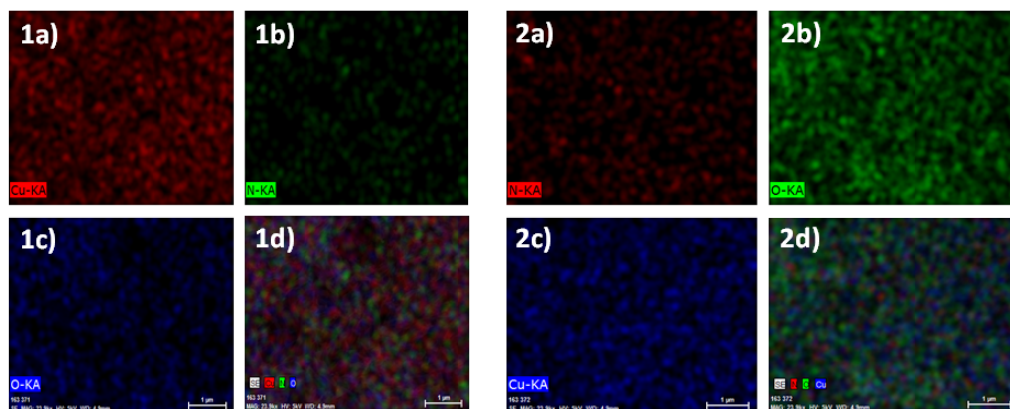


Figure S10. FESEM elemental analysis of Cu-MOG before (1) and after (2) catalysis

Table S1. Comparison of catalytic activity of present catalyst, Cu-MOG with the reported systems for the CuAAC reaction

Catalyst	Time (h)	mol%	Yield (%)	TOF (h ⁻¹)	References
Cu-MOG	6	2	91 ^a	7.58	This work
Cu-MOG	6	2	89 ^b	7.41	This work
Cu(I).3 gel	18	1	97 ^a	5.38	1
Cu(I).3 gel	18	1	92 ^b	5.11	1
MOF-1	12	1	99 ^a	8.25	2
MOF-2	12	1	40 ^a	3.33	2

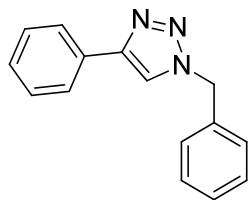
^aBenzyl azide & phenyl acetylene, ^bbenzyl azide & *p*-tolylacetylene as reactant.

Table S2. Comparison of gas adsorption behaviour of the Cu-MOG with reported metal xerogels

MOGs	N₂ uptake (cc/gm)	CO₂ uptake (cc/gm)	References
Cu-MOG	122	14	This work
BPPTP-Copper triflate gel	62	8	3
Ca-5TIA gel	—	32	4
Al-TCPE gel	170	—	5
TPPBT-Silver nitrate gel	29	—	6
MOG-1	58.95	—	7
MOG-2	29.21	—	7
MOG-3	18.90	—	7
MOG-4	9.15	—	7

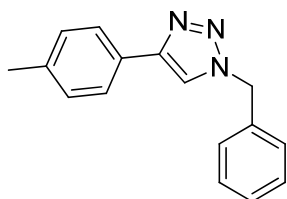
Characterization Data of the Products

Except for the product of Table 2, entry 12 & 13, all the other products are known compounds.



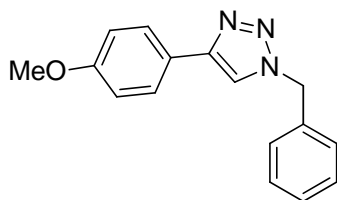
1-benzyl-4-phenyl-1H-1,2,3-triazole⁸ (Table 2, entry 1): White solid;

Yield: 94%; ¹H NMR (400 MHz, CDCl₃) δ 7.80 (m, 2H), 7.67 (s, 1H), 7.40–7.36 (m, 5H), 7.32–7.29 (m, 3H), 5.55 (s, 2H). ¹³C NMR (100 MHz, CDCl₃) δ 148.3, 134.8, 130.6, 129.3, 128.9, 128.9, 128.3, 128.2, 125.8, 119.7, 54.3.



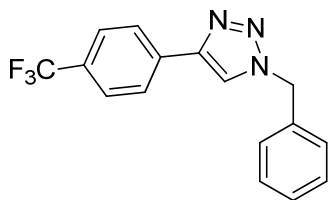
1-benzyl-4-(p-tolyl)-1H-1,2,3-triazole⁹ (Table 2, entry 2): White solid;

Yield: 94%; ¹H NMR (400 MHz, CDCl₃) δ 7.69–7.62 (m, 3H), 7.38–7.29 (m, 5H), 7.21–7.19 (m, 2H), 5.55 (s, 2H), 2.36 (s, 3H); ¹³C NMR (100 MHz, CDCl₃) δ 148.4, 138.1, 134.9, 129.6, 129.2, 128.8, 128.2, 127.8, 125.7, 119.3, 54.3, 21.4.



1-benzyl-4-(4-methoxyphenyl)-1H-1,2,3-triazole⁸ (Table 2, entry

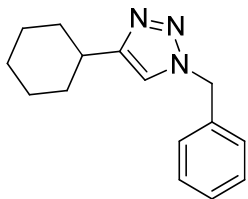
3): White solid; Yield: 90%; ¹H NMR (400 MHz, CDCl₃) δ 7.73–7.71 (m, 2H), 7.57 (s, 1H), 7.37 (m, 3H), 7.31–7.30 (m, 2H), 6.94–6.92 (m, 2H), 5.56 (s, 2H), 3.83 (s, 3H). ¹³C NMR (100 MHz, CDCl₃) δ 159.7, 148.2, 134.9, 129.2, 128.8, 128.1, 127.1, 123.4, 118.8, 114.3, 55.4, 54.3.



1-benzyl-4-(4-(trifluoromethyl)phenyl)-1H-1,2,3-triazole⁸ (Table 2,

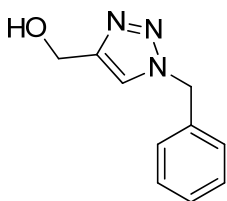
entry 4): White solid; Yield: 76%; ¹H NMR (400 MHz, CDCl₃) δ 7.91–7.89 (m, 2H), 7.76 (s,

1H), 7.64–7.62 (m, 2H), 7.42–7.38 (m, 3H), 7.35–7.30 (m, 2H), 5.57 (s, 2H). ¹³C NMR (100 MHz, CDCl₃) δ 146.9, 134.5, 134.1, 130.2 (q, *J* = 32.3 Hz), 129.4, 129.1, 128.2, 126.0, 125.9 (q, *J* = 3.7 Hz), 125.6 (q, *J* = 270.3 Hz), 120.4, 54.5.



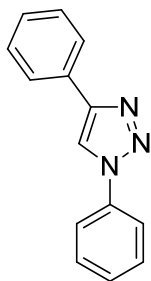
1-benzyl-4-cyclohexyl-1H-1,2,3-triazole⁸ (Table 2, entry 5): White solid;

Yield: 76%; ¹H NMR (400 MHz, CDCl₃) δ 7.37–7.34 (m, 3H), 7.26–7.24 (m, 2H), 7.13 (s, 1H), 5.48 (s, 2H), 2.74–2.73 (m, 1H), 2.03–2.01 (m, 2H), 1.77 (m, 2H), 1.70 (m, 1H), 1.39–1.31 (m, 4H), 1.22 (m, 1H). ¹³C NMR (100 MHz, CDCl₃) δ 154.3, 135.1, 129.1, 128.7, 128.1, 119.3, 54.1, 35.4, 33.1, 32.9, 26.2, 26.1.



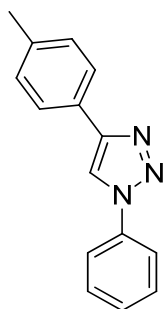
(1-benzyl-1H-1,2,3-triazol-4-yl)methanol⁸ (Table 2, entry 6): White solid;

Yield: 51%; ¹H NMR (400 MHz, CDCl₃) δ 7.44 (s, 1H), 7.38–7.34 (m, 3H), 7.27–7.25 (m, 2H), 5.50 (d, *J* = 4.0 Hz, 2H), 4.75 (s, 2H); ¹³C NMR (100 MHz, CDCl₃) δ 148.2, 134.6, 129.2, 128.9, 128.2, 121.7, 56.6, 54.3.

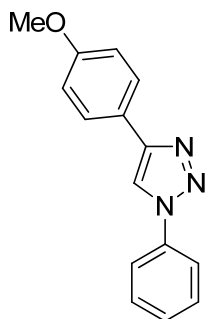


1,4-diphenyl-1H-1,2,3-triazole¹⁰ (Table 2, entry 7): White solid; Yield: 53%; ¹H

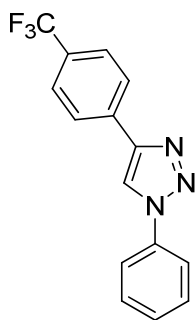
NMR (400 MHz, CDCl₃) δ 8.21 (s, 1H), 7.92 (d, *J* = 7.2 Hz, 2H), 7.81 (d, *J* = 8 Hz, 2H), 7.55 (t, *J* = 8 Hz, 2H), 7.48–7.44 (m, 3H), 7.39–7.35 (m, 1H); ¹³C NMR (100 MHz, CDCl₃) δ 148.5, 137.2, 130.3, 129.9, 129.1, 128.9, 128.6, 126.0, 120.7, 117.7.



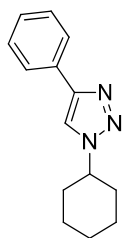
1-phenyl-4-(p-tolyl)-1H-1,2,3-triazole¹⁰ (Table 2, entry 8): White solid; Yield: 53%; ¹H NMR (400 MHz, CDCl₃) δ 8.15 (s, 1H), 7.80 (m, 4H), 7.56 (t, *J* = 7.6 Hz, 2H), 7.46 (t, *J* = 7.6 Hz, 1H), 7.27 (s, 2H), 2.39 (s, 3H); ¹³C NMR (100 MHz, CDCl₃) δ 148.8, 138.4, 137.5, 129.9, 129.7, 128.8, 127.8, 125.9, 120.6, 117.4, 21.4.



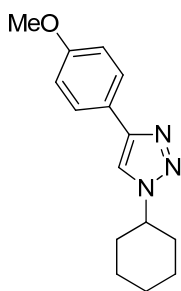
4-(4-methoxyphenyl)-1-phenyl-1H-1,2,3-triazole¹⁰ (Table 2, entry 9): White solid; Yield: 56%; ¹H NMR (400 MHz, CDCl₃) δ 8.10 (s, 1H), 7.84 (d, *J* = 8.8 Hz, 2H), 7.78-7.76 (m, 2H), 7.54 (t, *J* = 7.6 Hz, 2H), 7.45-7.41 (m, 1H), 6.99 (d, *J* = 8.8 Hz, 2H), 3.84 (s, 3H); ¹³C NMR (100 MHz, CDCl₃) δ 159.9, 148.4, 137.2, 129.9, 128.8, 127.3, 123.1, 120.6, 116.9, 114.4, 55.5.



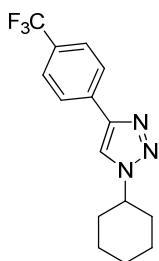
1-phenyl-4-(4-(trifluoromethyl)phenyl)-1H-1,2,3-triazole¹¹ (Table 2, entry 10): White solid; Yield: 52%; ¹H NMR (400 MHz, CDCl₃) δ 9.48 (s, 1H), 8.17 (d, 2H, *J* = 8.0 Hz), 7.96 (d, 2H, *J* = 8.4 Hz), 7.88 (d, 2H, *J* = 8 Hz), 7.66 (t, 2H, *J* = 7.6 Hz), 7.54 (br s, 1H); ¹³C NMR (100 MHz, DMSO-*d*₆) δ 146.3, 136.9, 134.7, 130.4, 129.4, 128.9 (q, *J*_{C-*CF*₃} = 31.8 Hz), 126.5 (q, *J*_{C-*CF*₃} = 3.8 Hz), 126.3, 126.0 (q, *J*_{C-*CF*₃} = 270.6 Hz), 121.4, 120.6.



1-cyclohexyl-4-phenyl-1H-1,2,3-triazole⁸ (Table 2, entry 11): White solid; Yield: 52%; ¹H NMR (400 MHz, CDCl₃) δ 7.84 (d, *J* = 7.6 Hz, 2H), 7.77 (s, 1H), 7.43 (m, 2H), 7.33 (m, 1H), 4.52 (tt, *J* = 12.0, 4.0 Hz, 1H), 2.26 (m, 2H), 1.95 (m, 2H), 1.83–1.75 (m, 3H), 1.48 (m, 2H), 1.32 (tt, *J* = 12.5, 3.5 Hz, 1H). ¹³C NMR (100 MHz, CDCl₃) δ 147.3, 130.9, 128.8, 127.9, 125.6, 117.2, 60.1, 33.6, 25.2, 25.1.

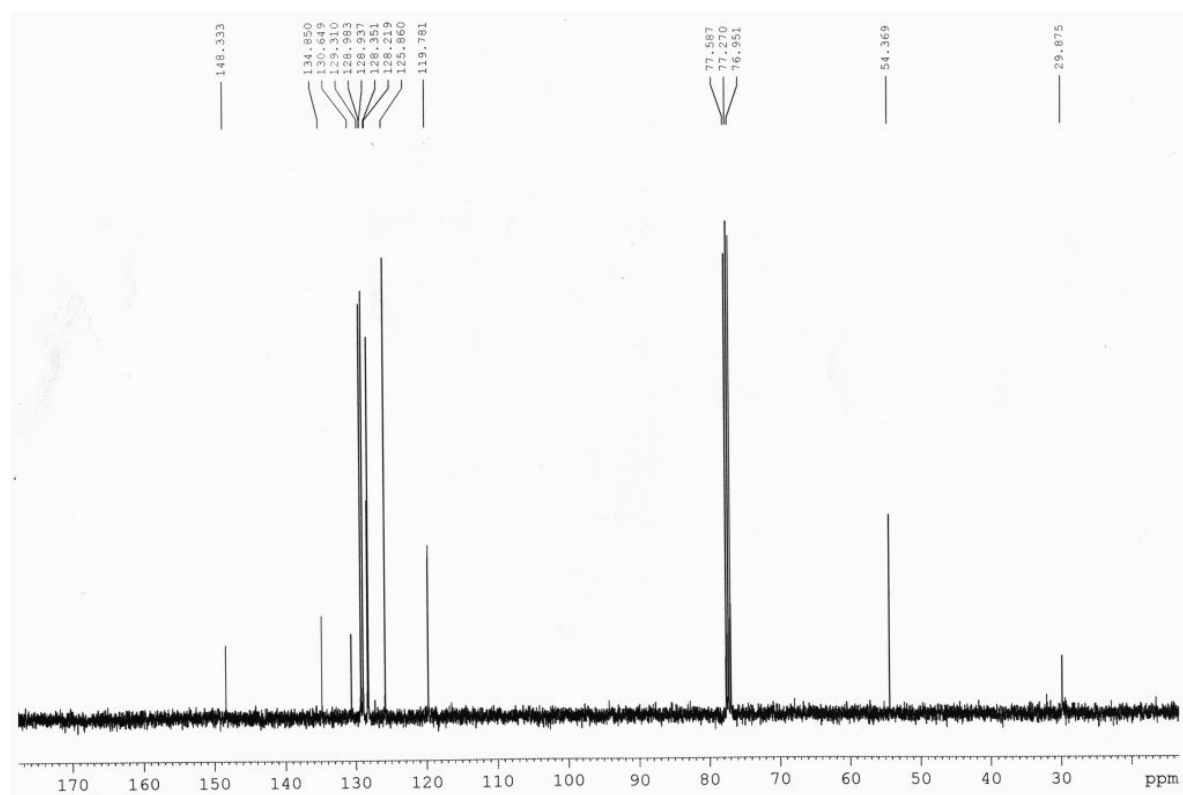
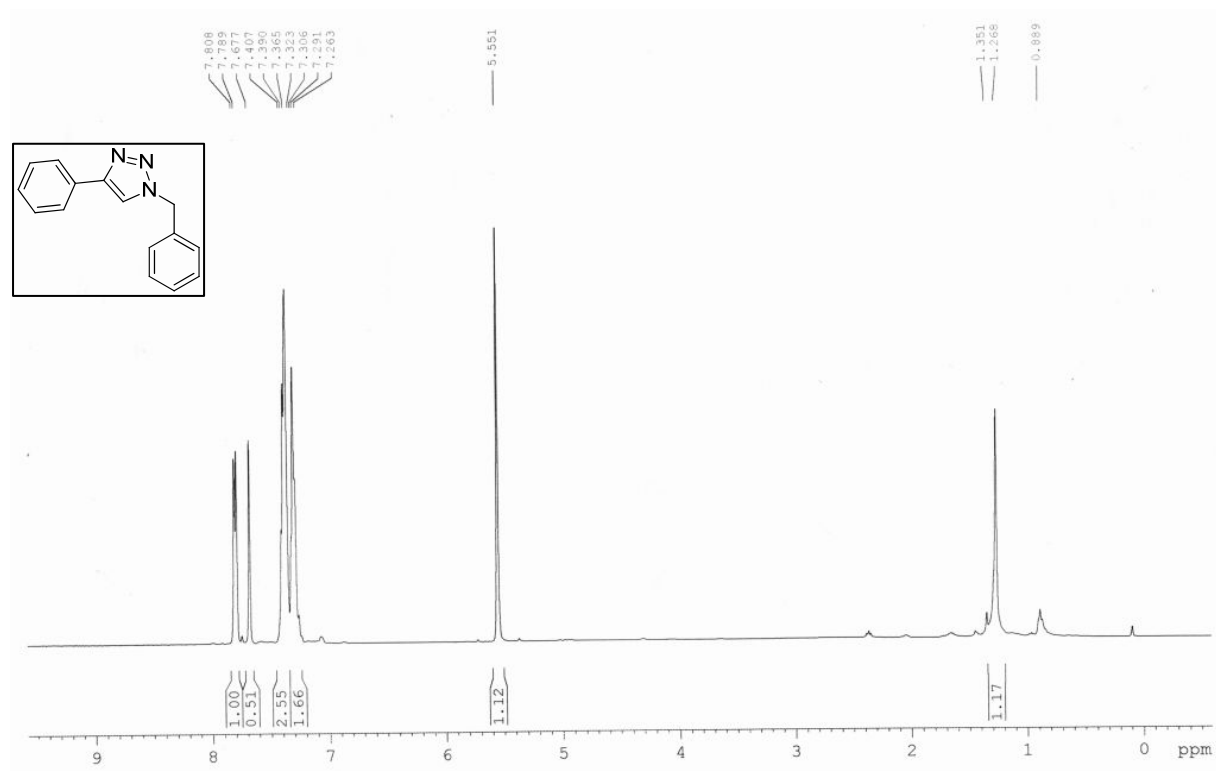


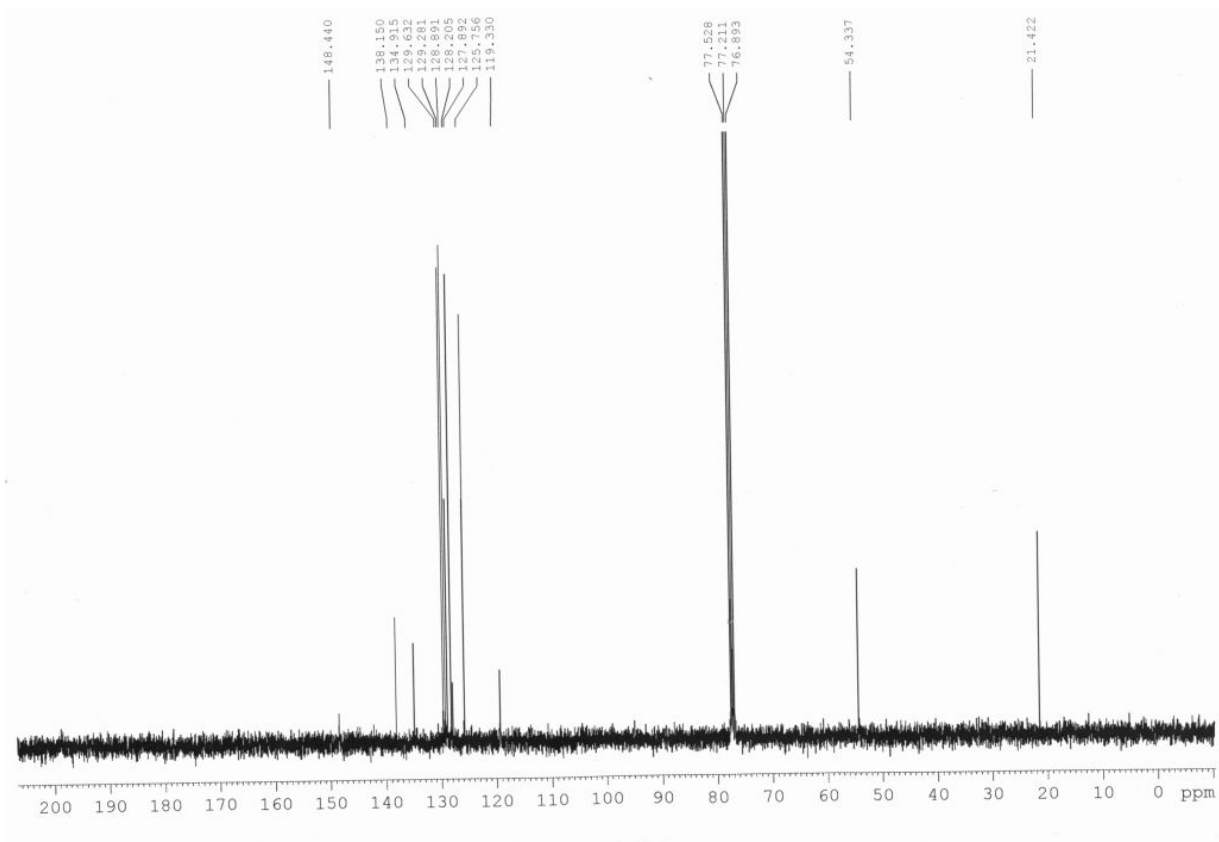
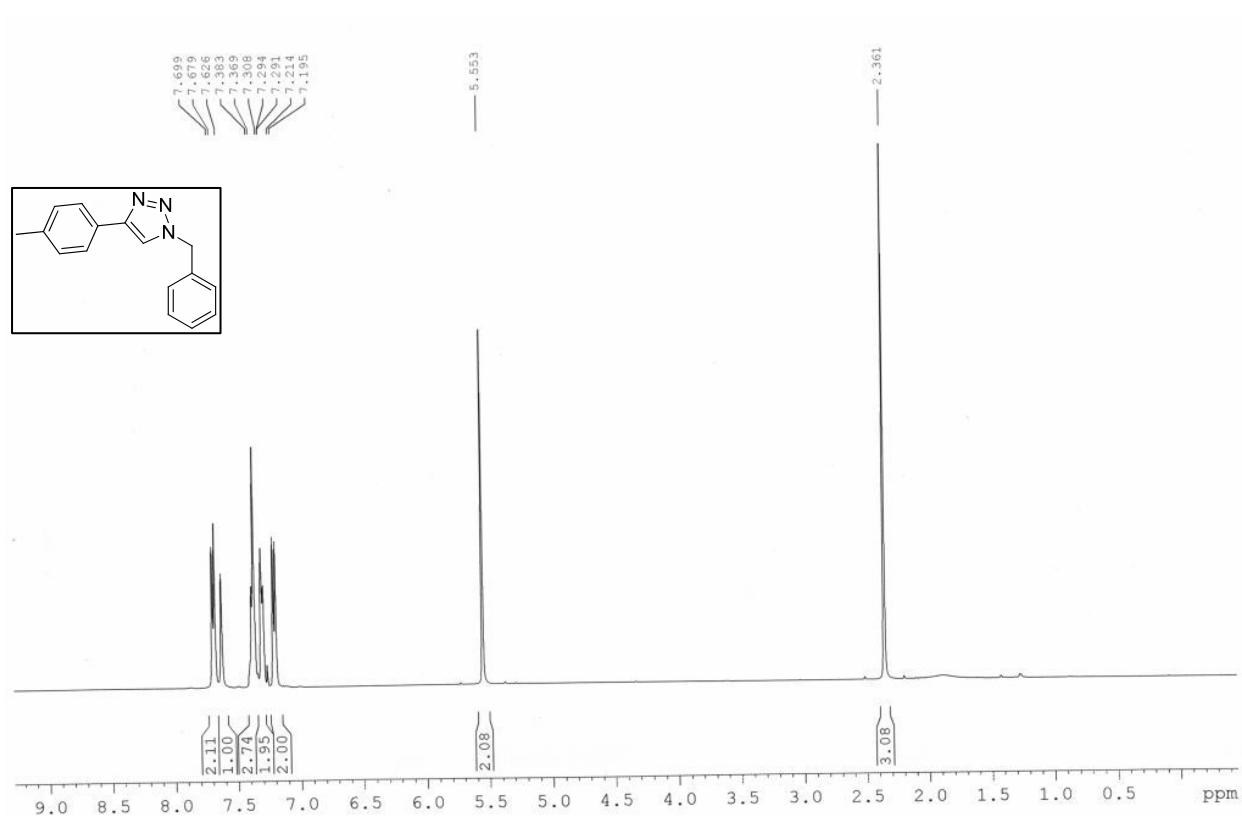
1-cyclohexyl-4-(4-methoxyphenyl)-1H-1,2,3-triazole (Table 2, entry 12): Light yellow solid; Yield: 52%; ¹H NMR (400 MHz, CDCl₃) δ 7.76 (d, *J* = 8.8 Hz, 2H), 7.67 (s, 1H), 6.95 (d, *J* = 8.8 Hz, 2H), 4.51 (m, 1H), 3.83 (s, 3H), 2.26–2.22 (m, 2H), 1.95–1.91 (m, 2H), 1.83–1.72 (m, 3H), 1.52–1.41 (m, 2H), 1.34–1.24 (m, 1H). ¹³C NMR (100 MHz, CDCl₃) δ 159.5, 147.0, 127.0, 123.3, 116.6, 114.2, 60.2, 55.3, 33.5, 25.2, 25.1. HRMS (ESI): *m/z* calcd for C₁₅H₂₀N₃O [M + H]⁺, 258.1606, found: 258.1601.

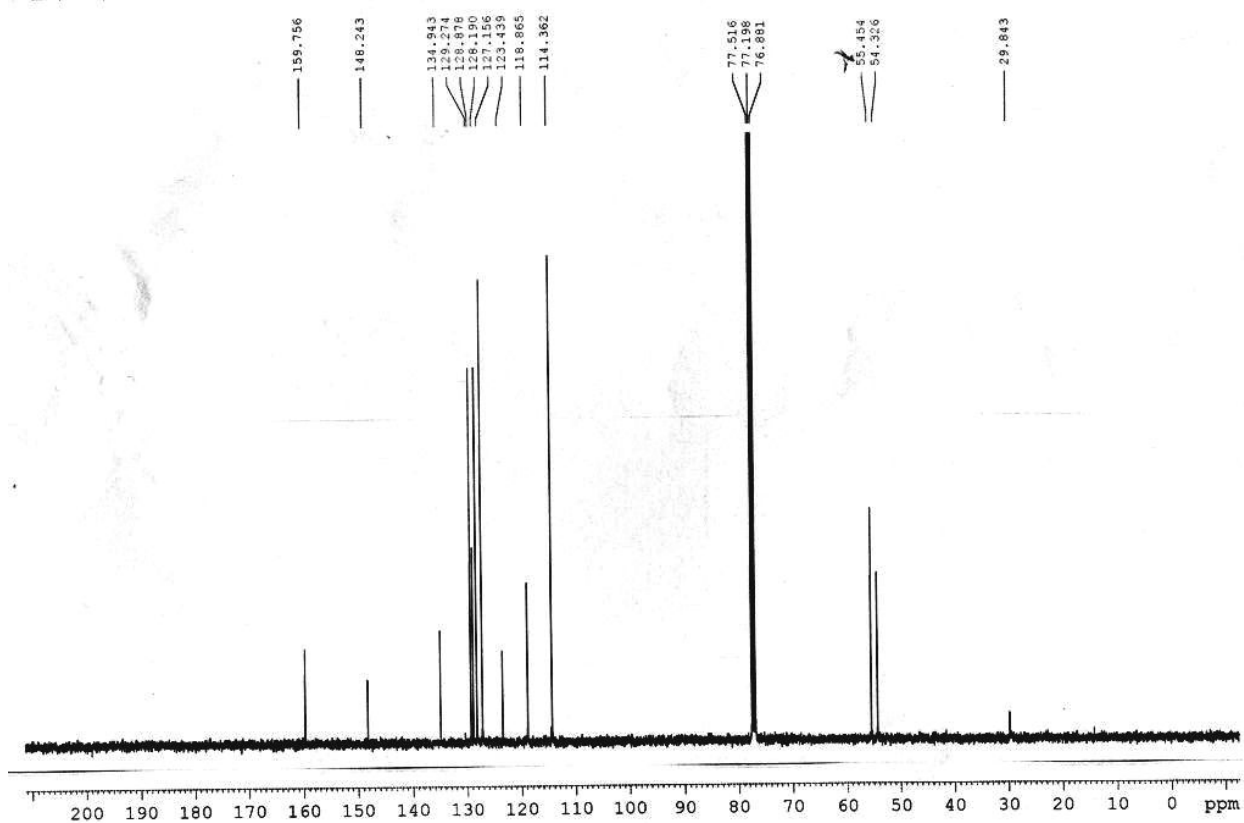
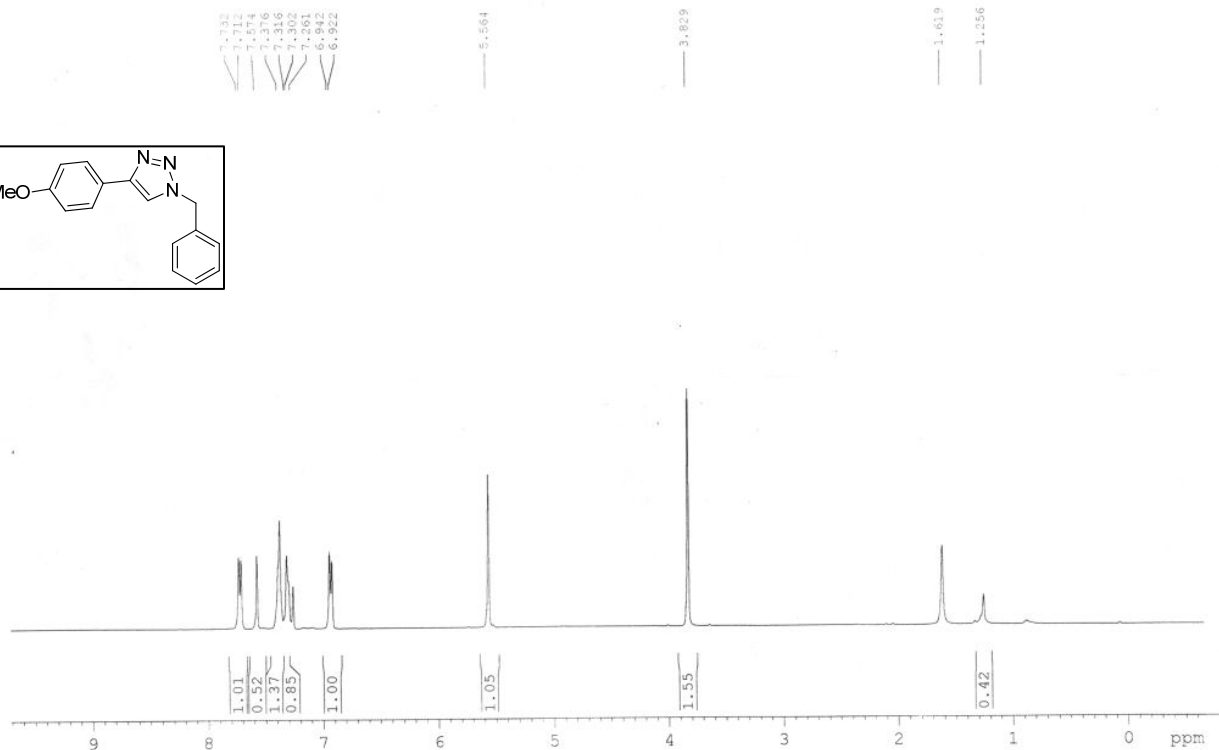
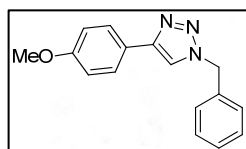


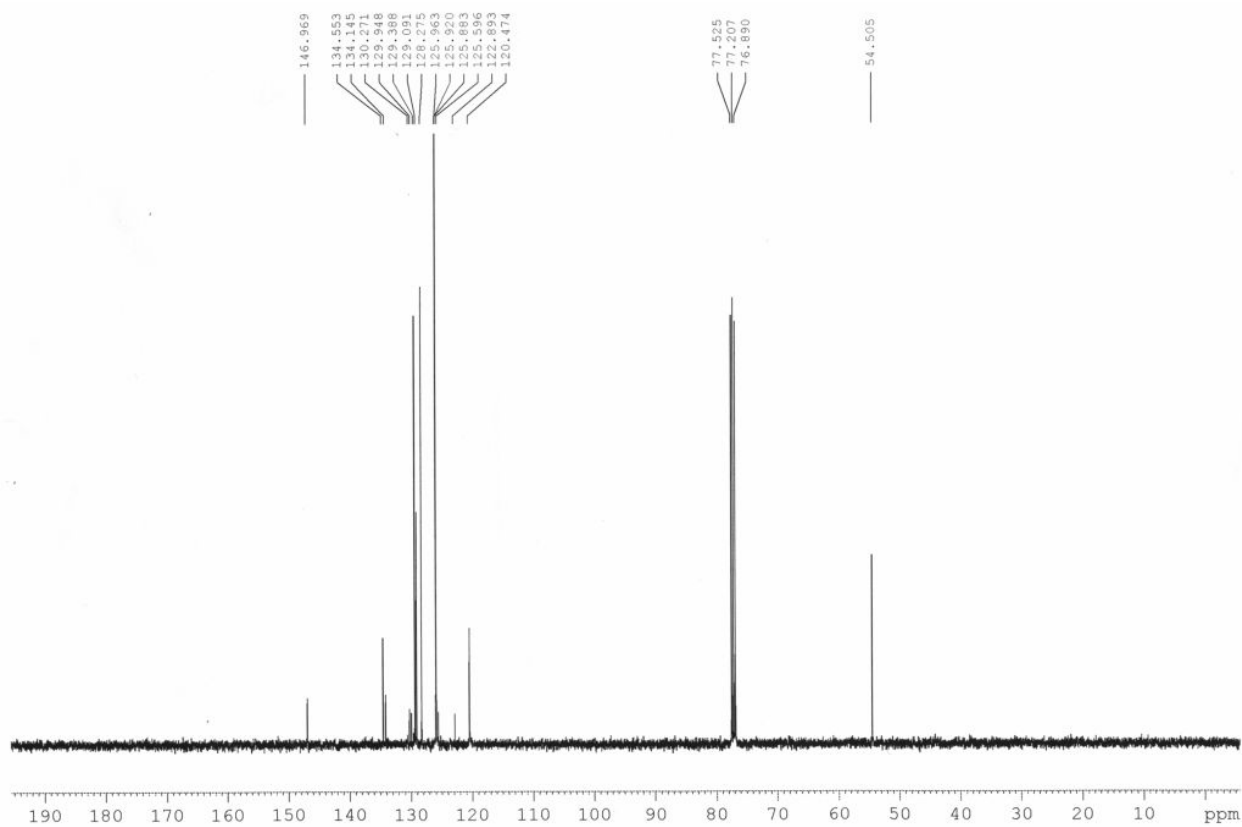
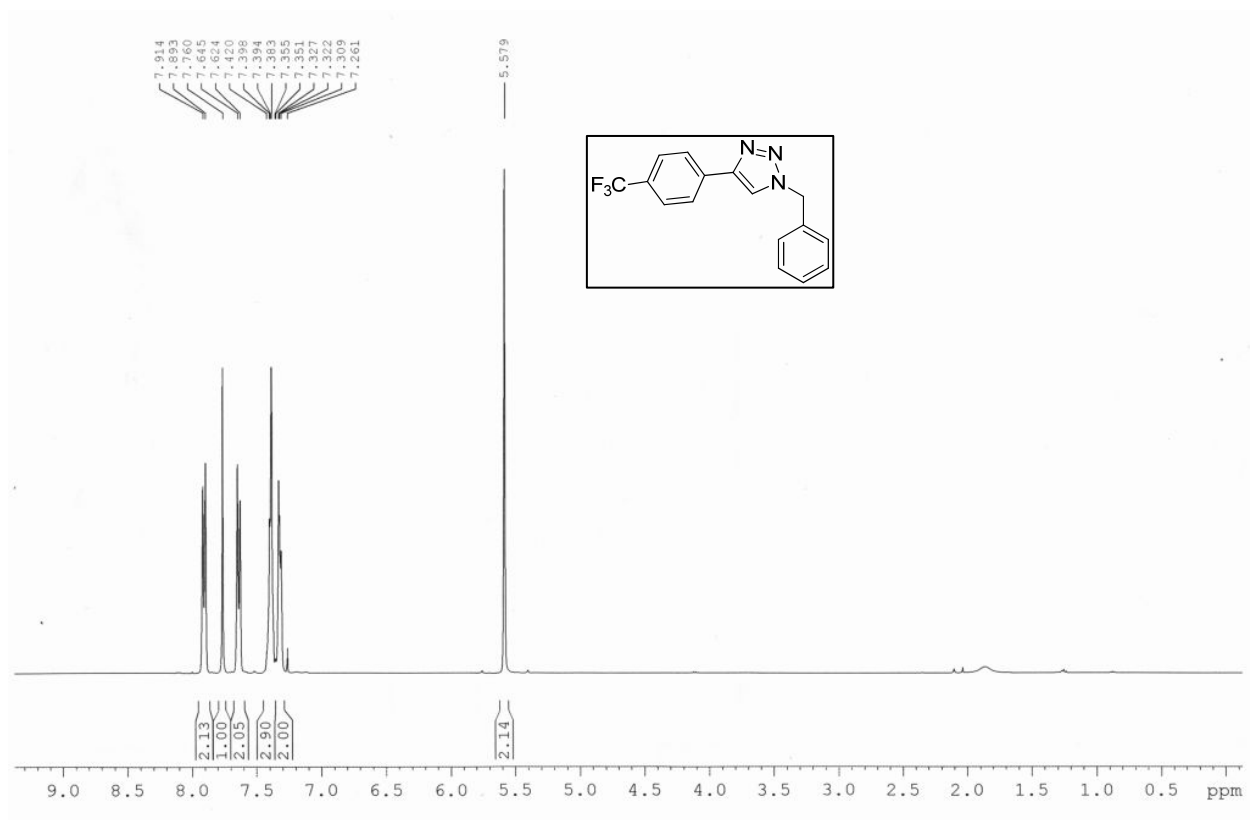
1-cyclohexyl-4-(4-(trifluoromethyl)phenyl)-1H-1,2,3-triazole (Table 2, entry 13): White solid; Yield: 52%; ¹H NMR (400 MHz, CDCl₃) δ 7.94 (d, *J* = 8.4 Hz, 2H), 7.85 (s, 1H), 7.65 (d, *J* = 8.4 Hz, 2H), 4.52–4.44 (m, 1H), 2.26–2.22 (m, 2H), 1.95–1.90 (m, 2H), 1.83–1.73 (m, 3H), 1.52–1.41 (m, 2H), 1.34–1.23 (m, 1H). ¹³C NMR (100 MHz, CDCl₃) δ 146.0, 134.5, 130.3 (q, *J*_{C-CF₃} = 32.3 Hz), 128.3, 125.9 (q, *J*_{C-CF₃} = 4.9 Hz), 125.6 (q, *J*_{C-CF₃} = 270.0 Hz), 118.3, 60.4, 33.7, 25.3, 25.2. HRMS (ESI): *m/z* calcd for C₁₅H₁₇N₃F₃ [M + H]⁺, 296.1375, found: 296.1361.

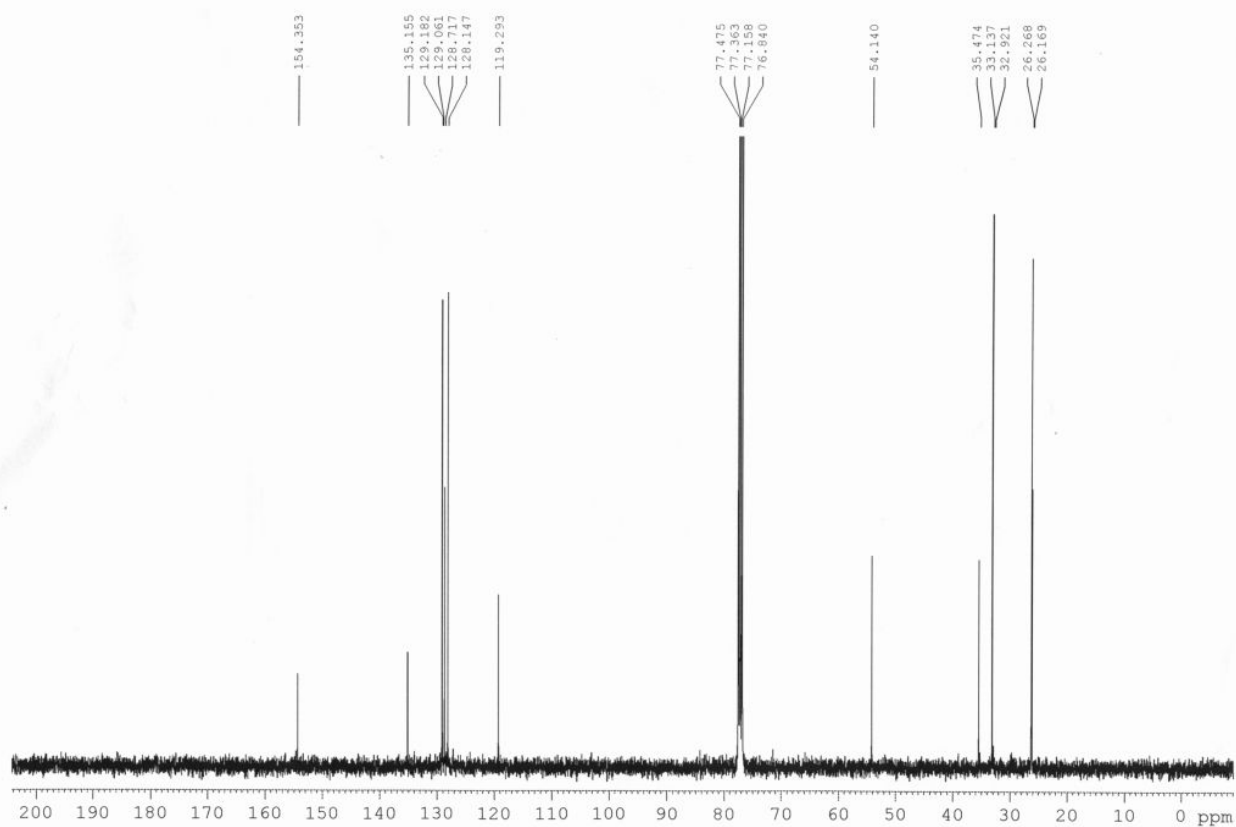
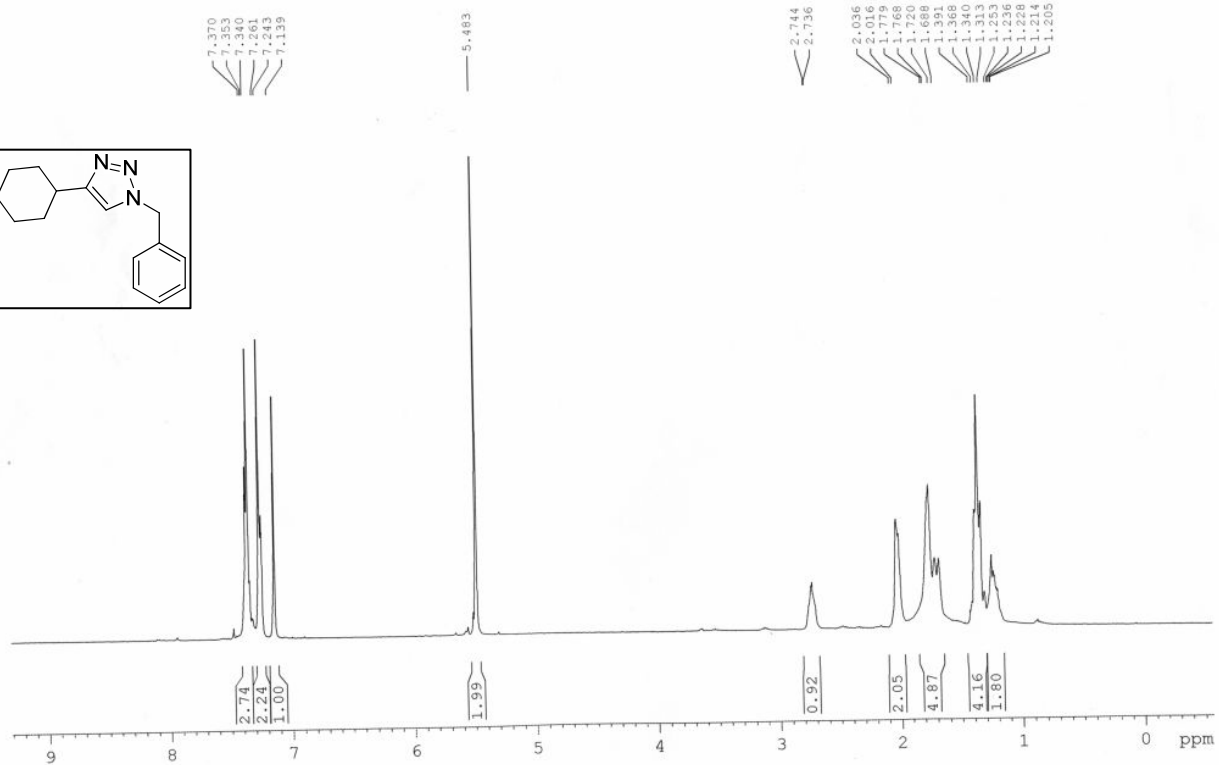
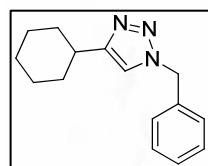
NMR Spectra (^1H , ^{13}C) (Products for CuAAC reaction)

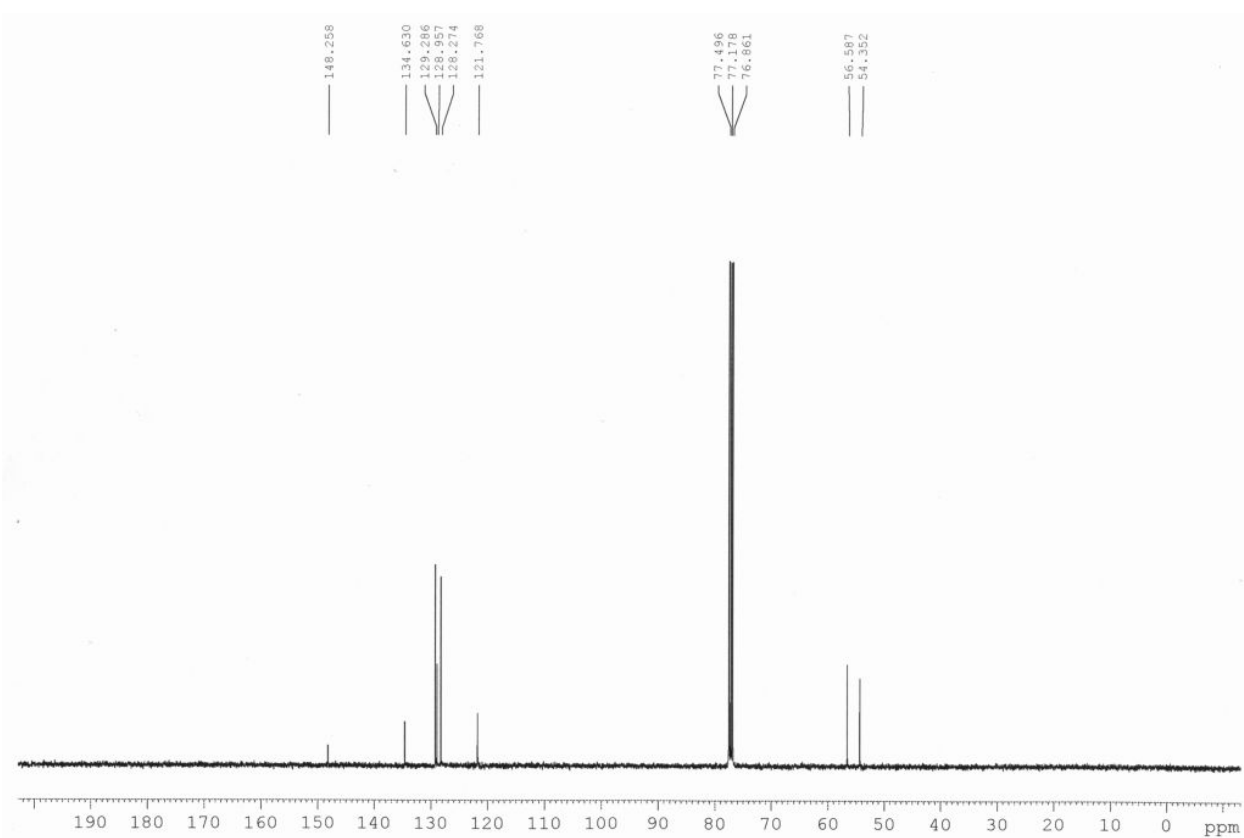
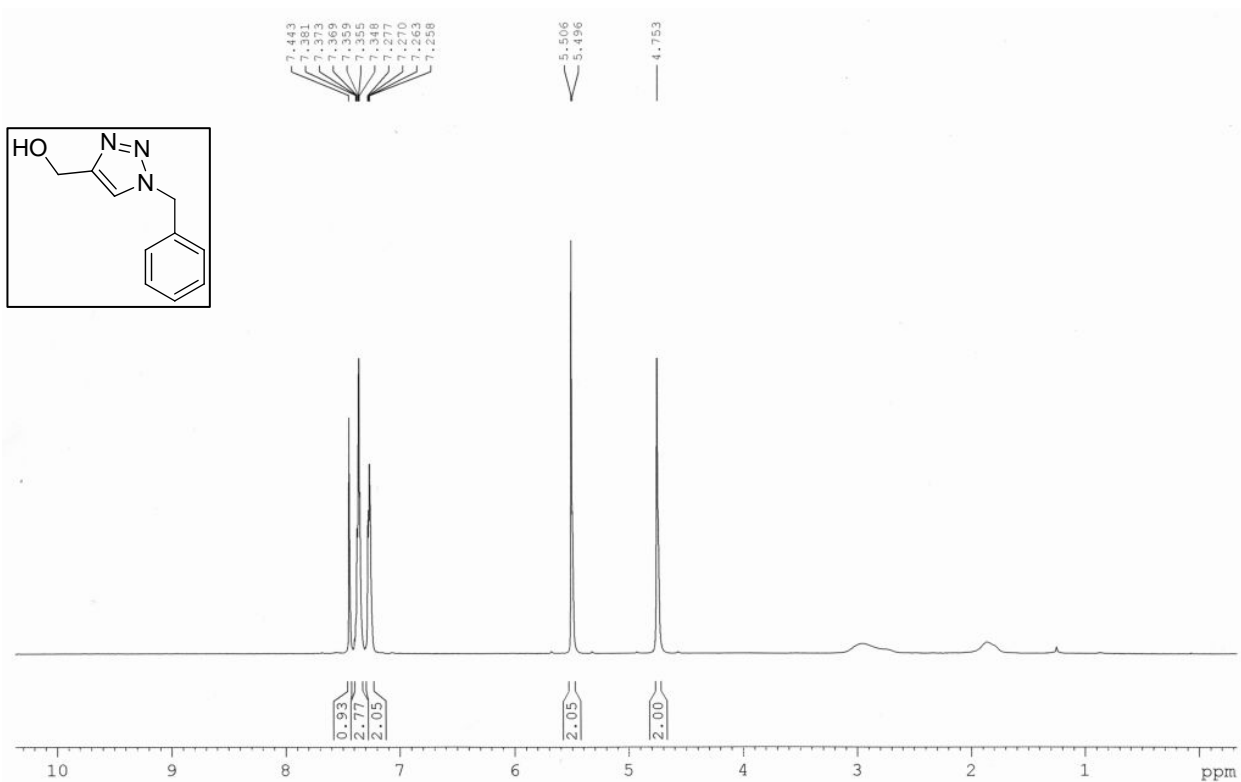
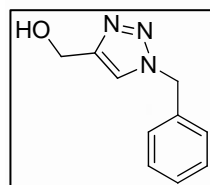


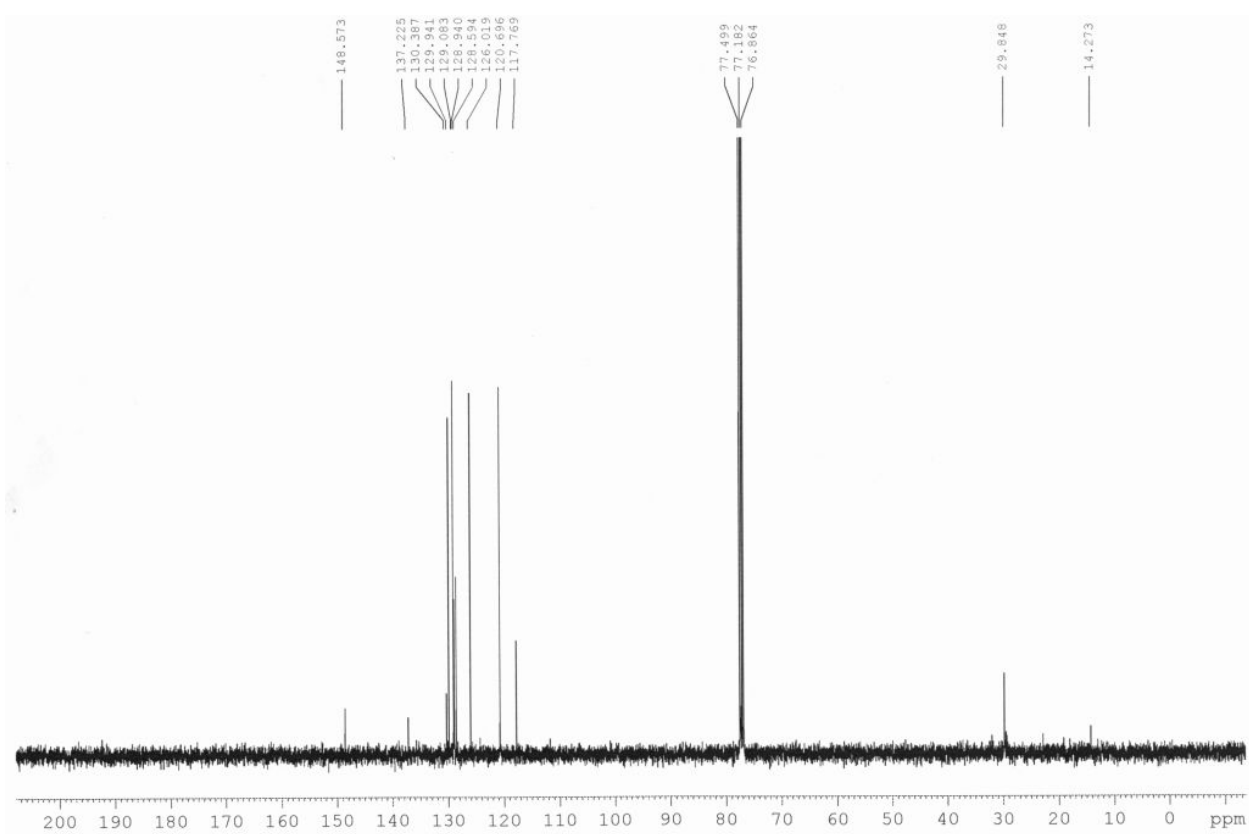
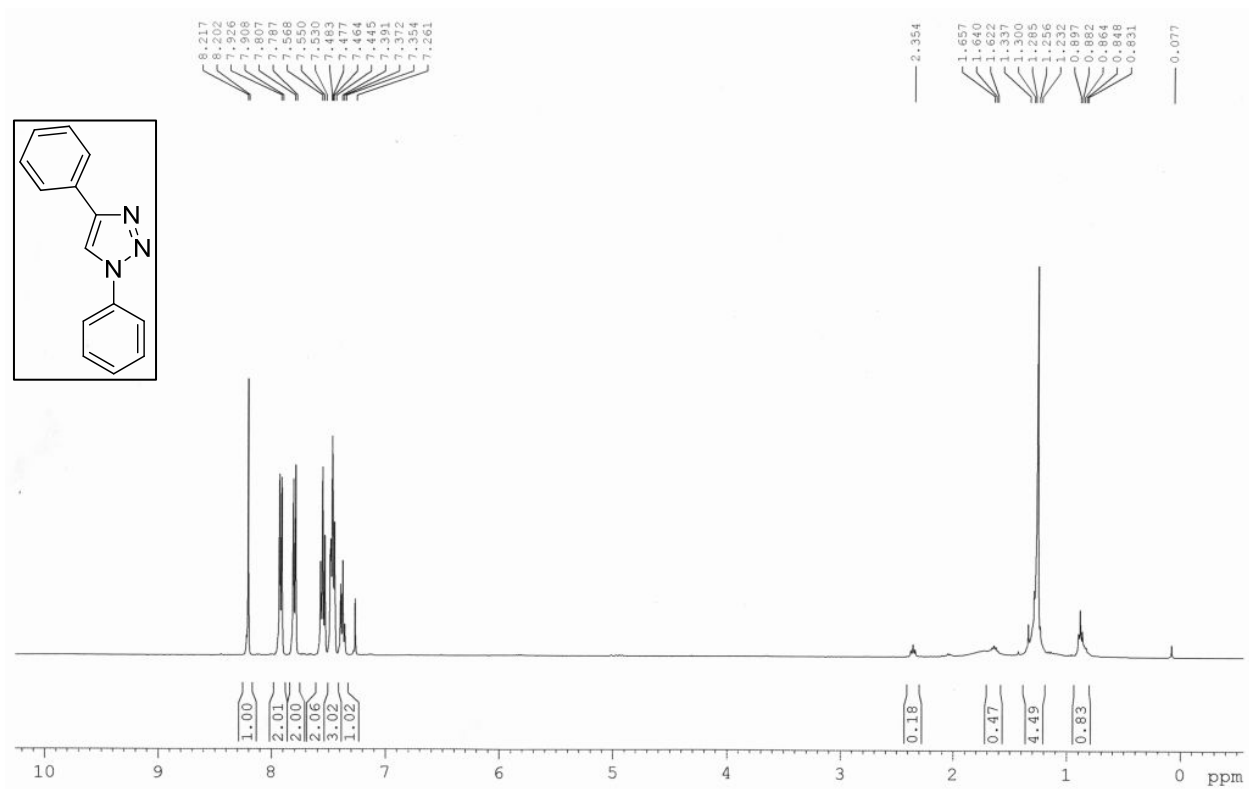


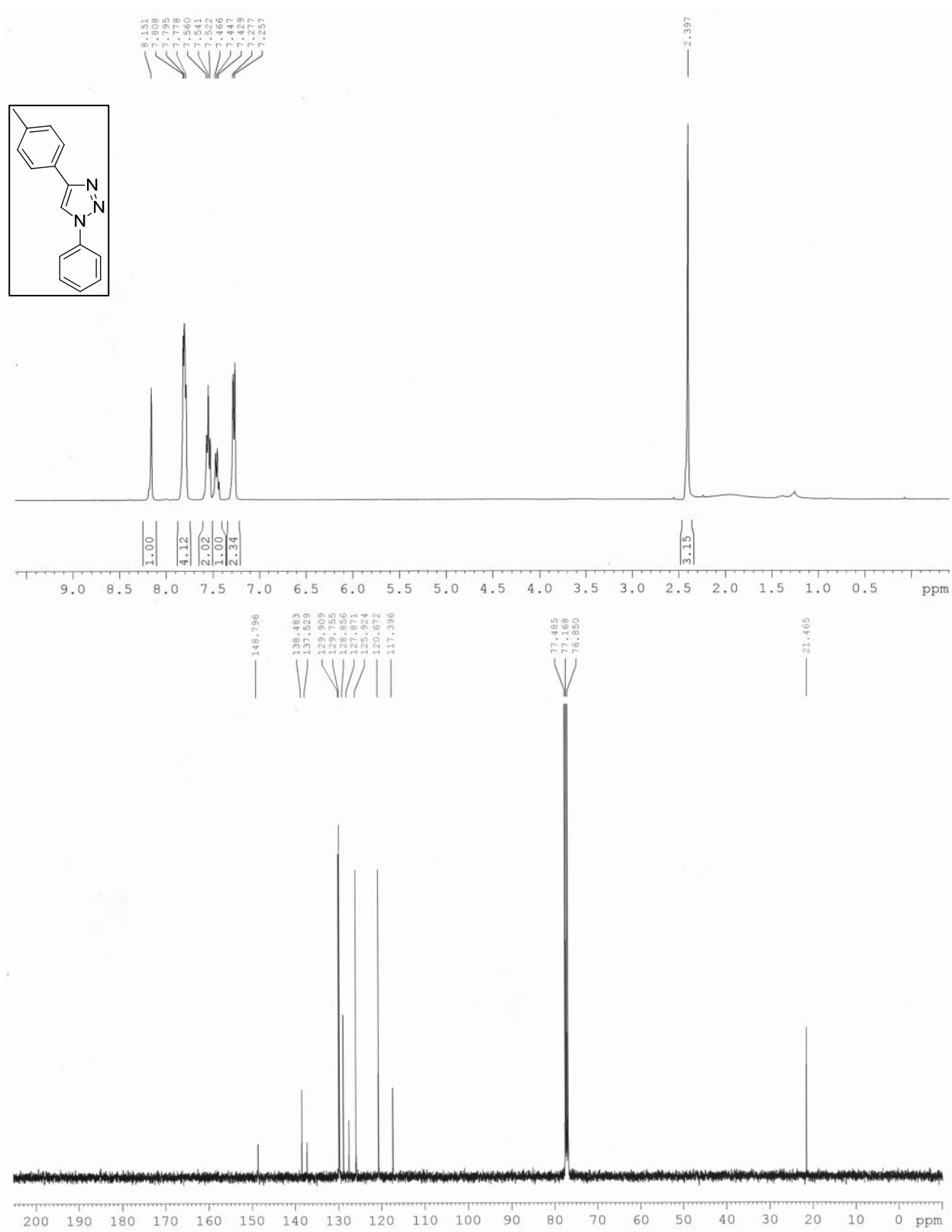


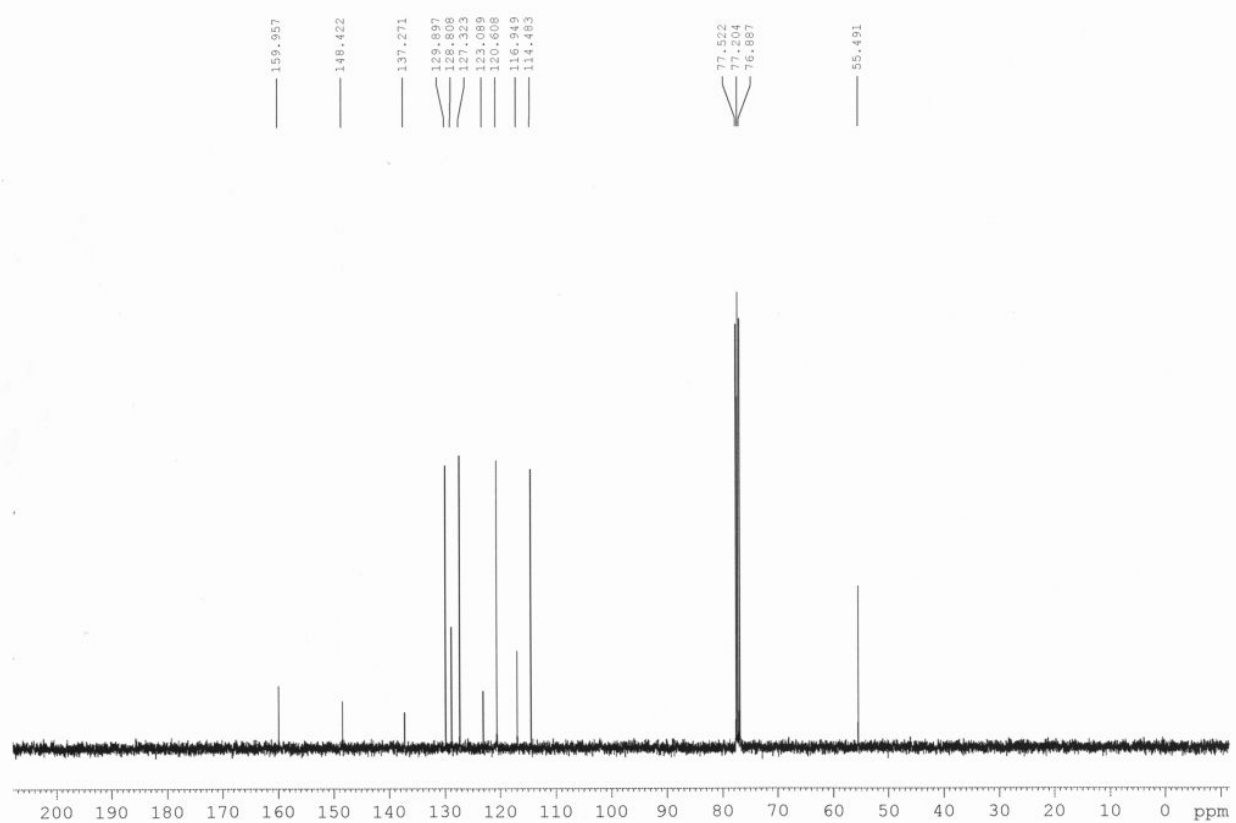
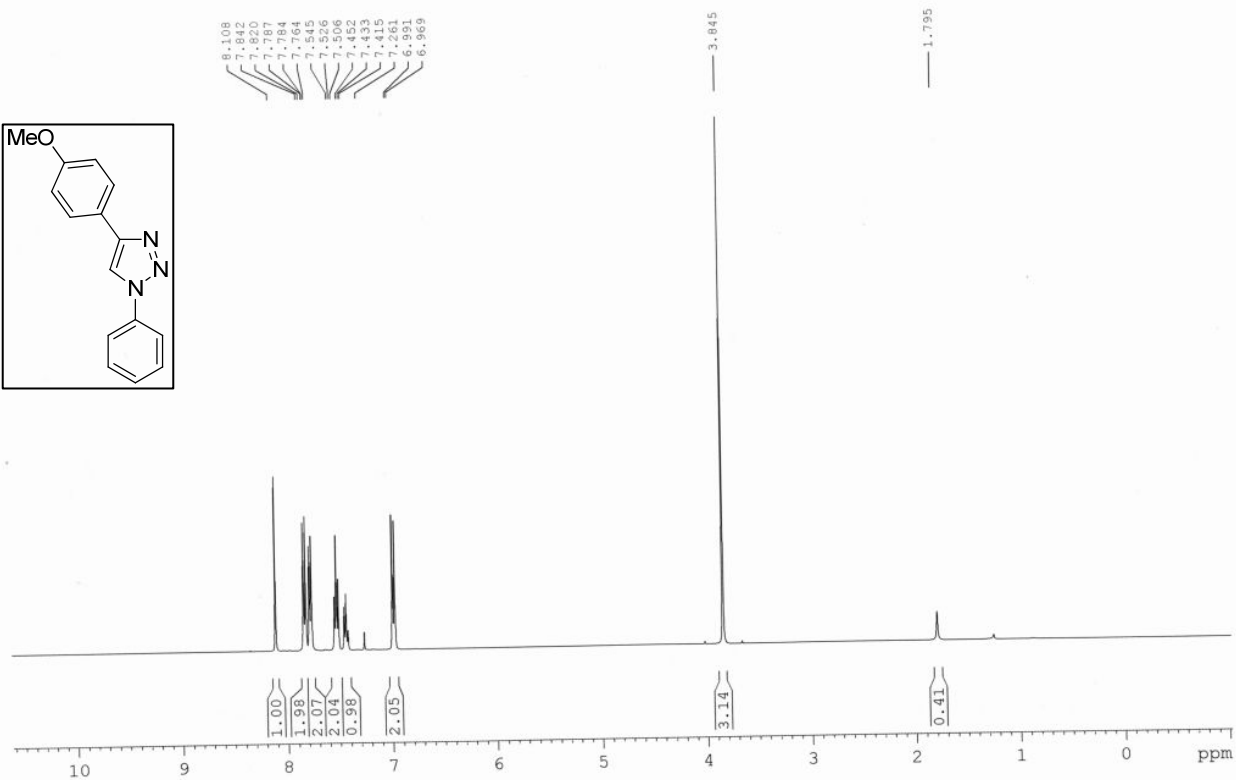
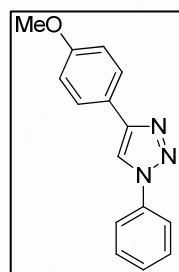


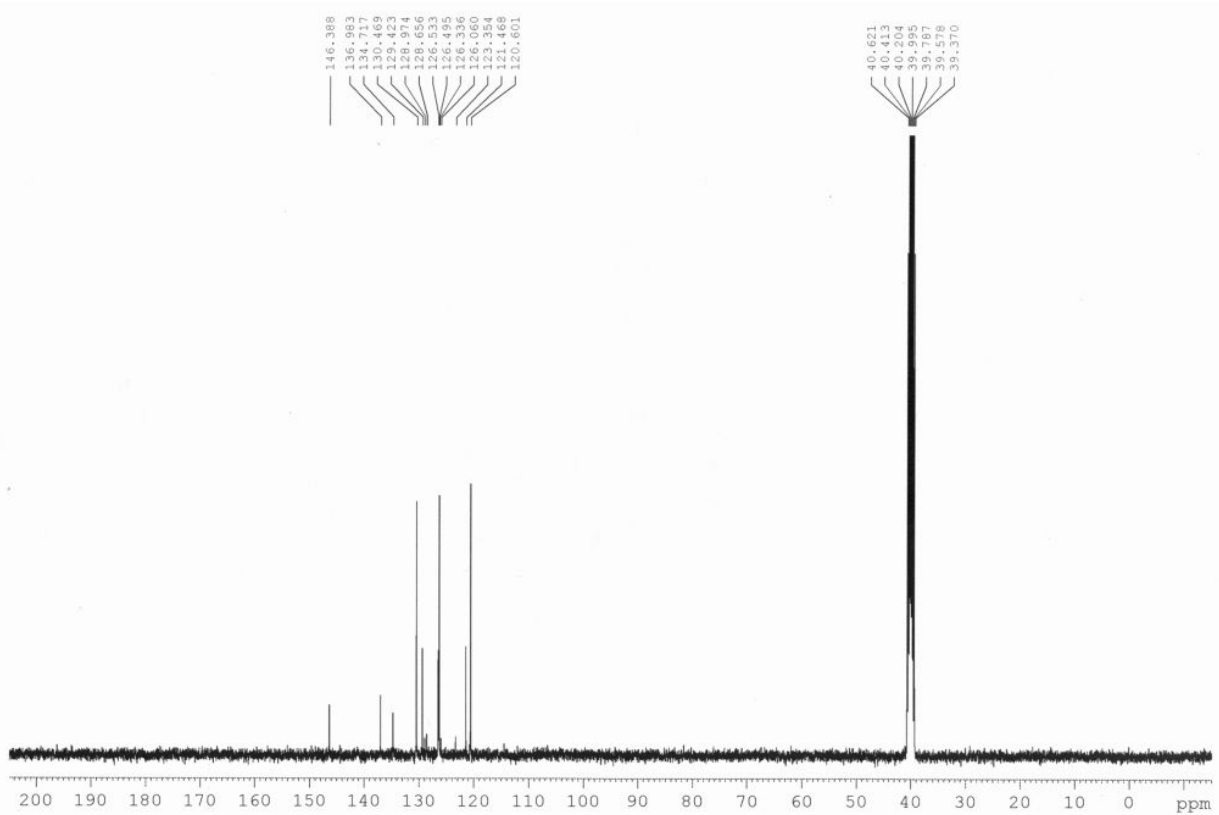
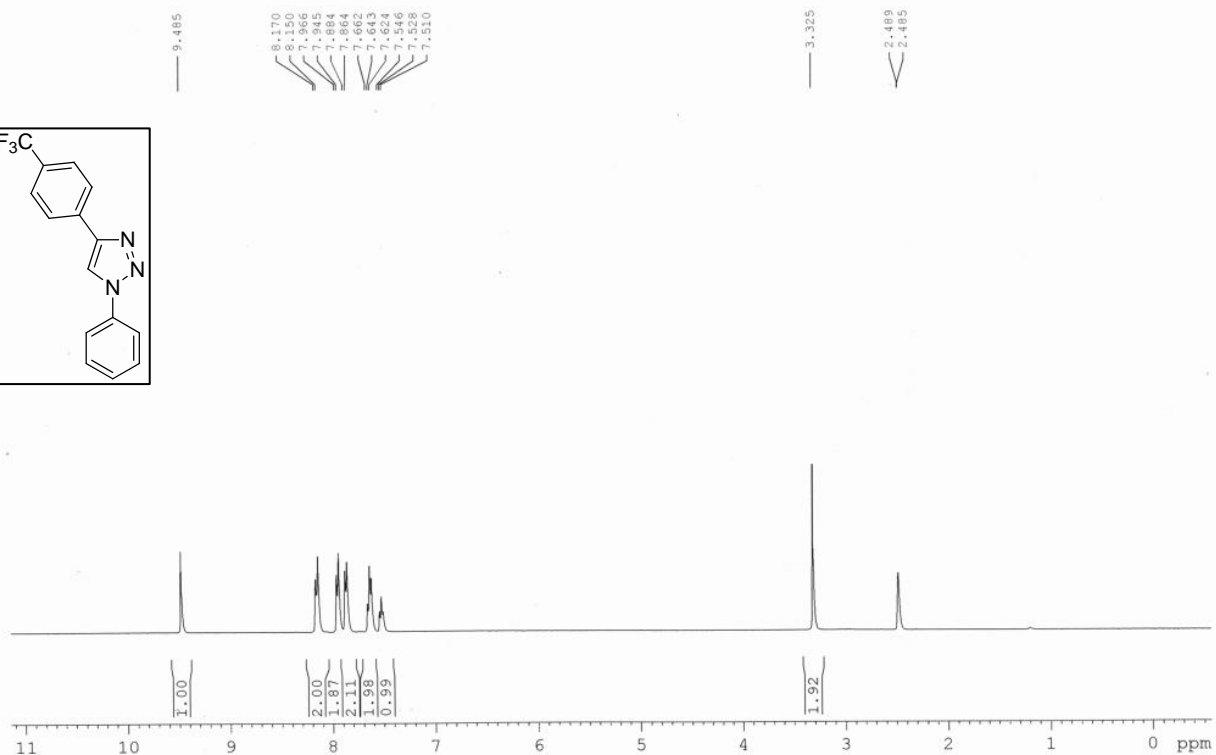
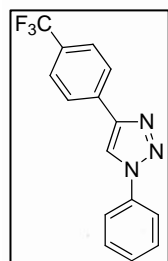


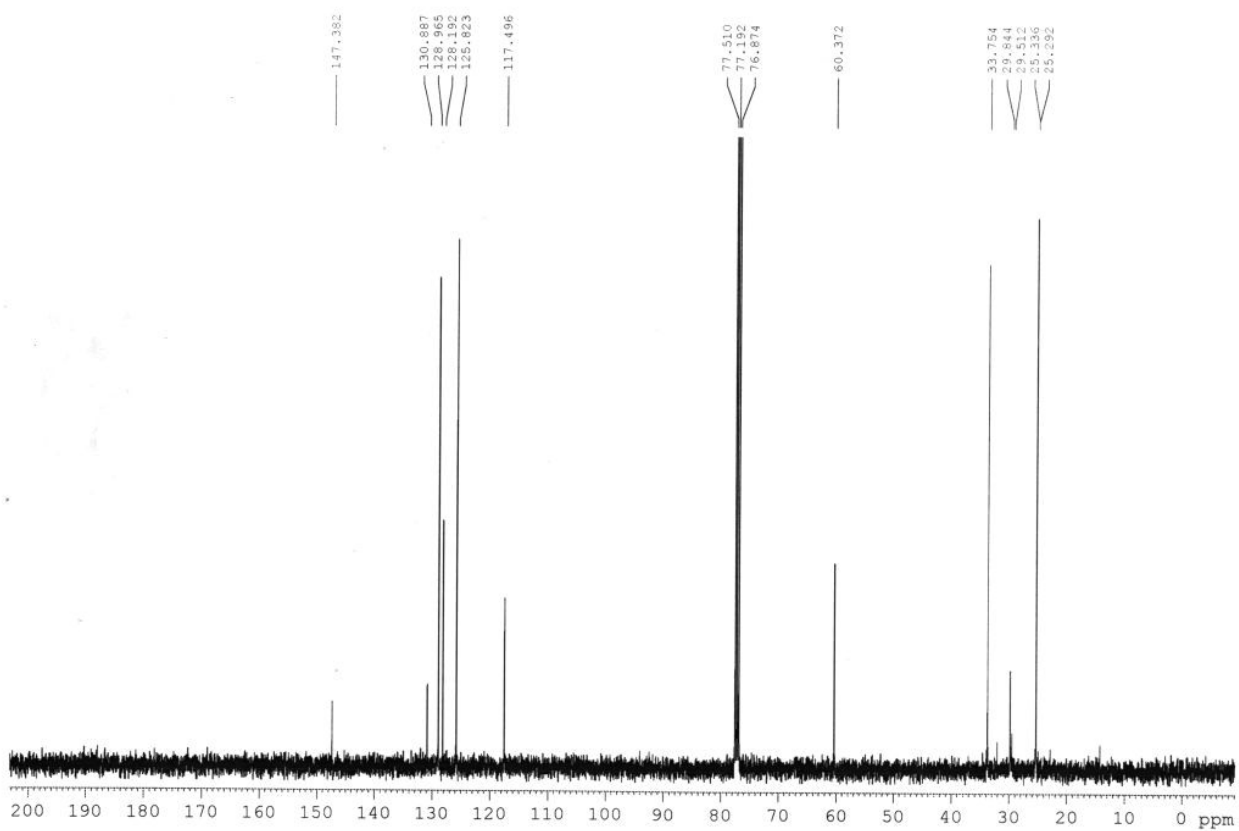
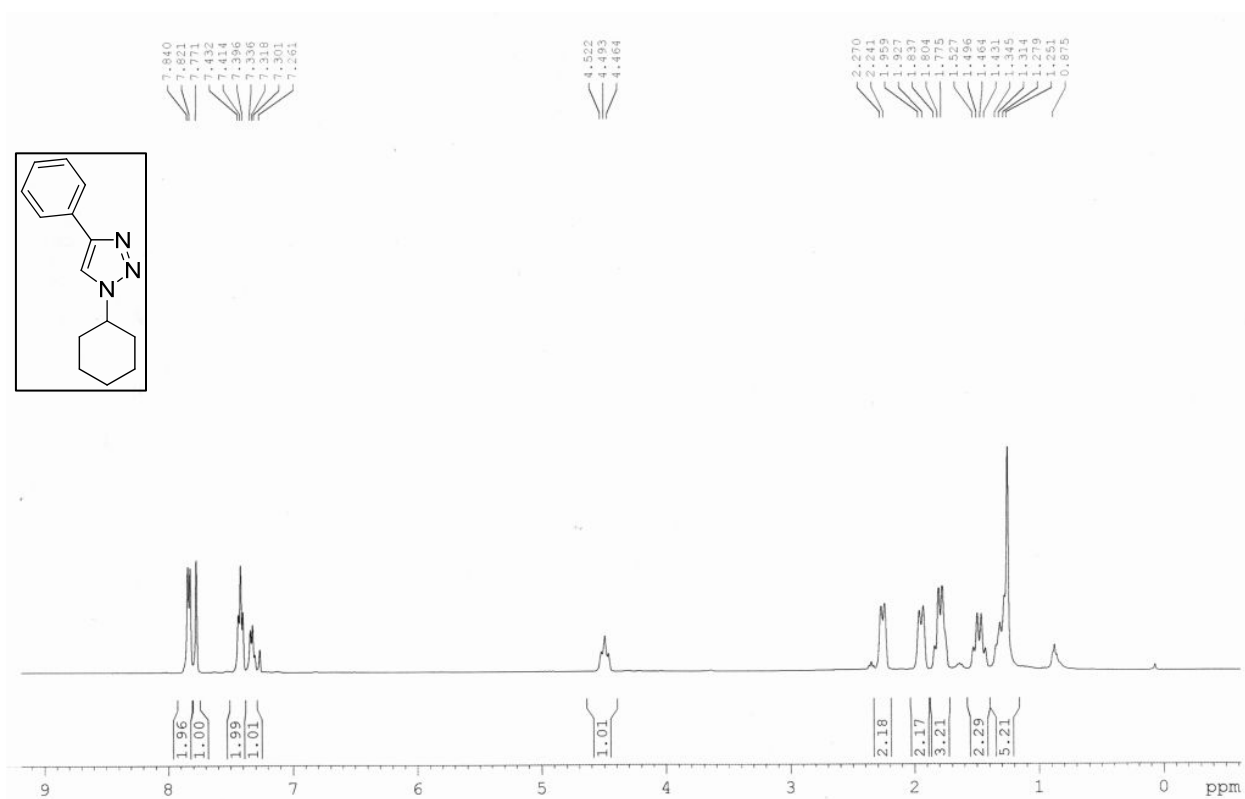
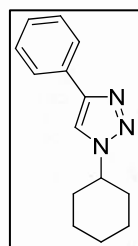


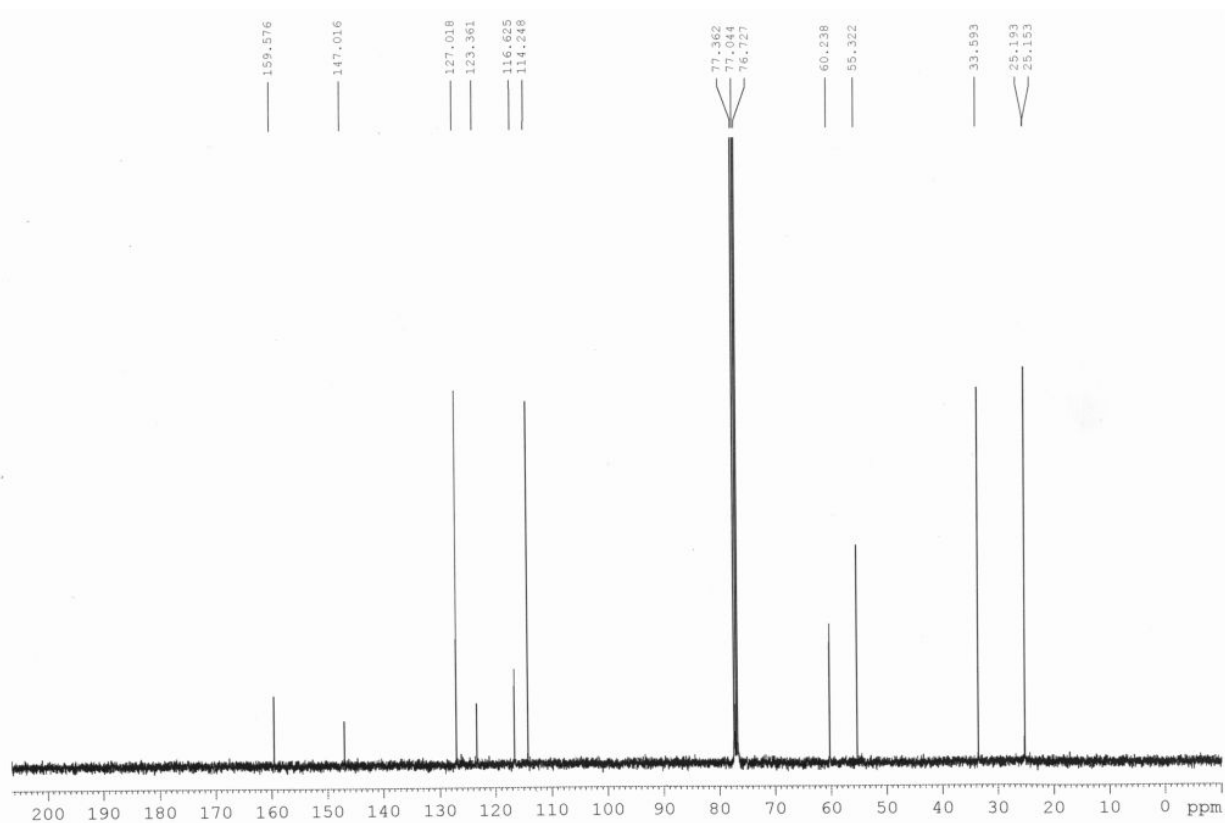
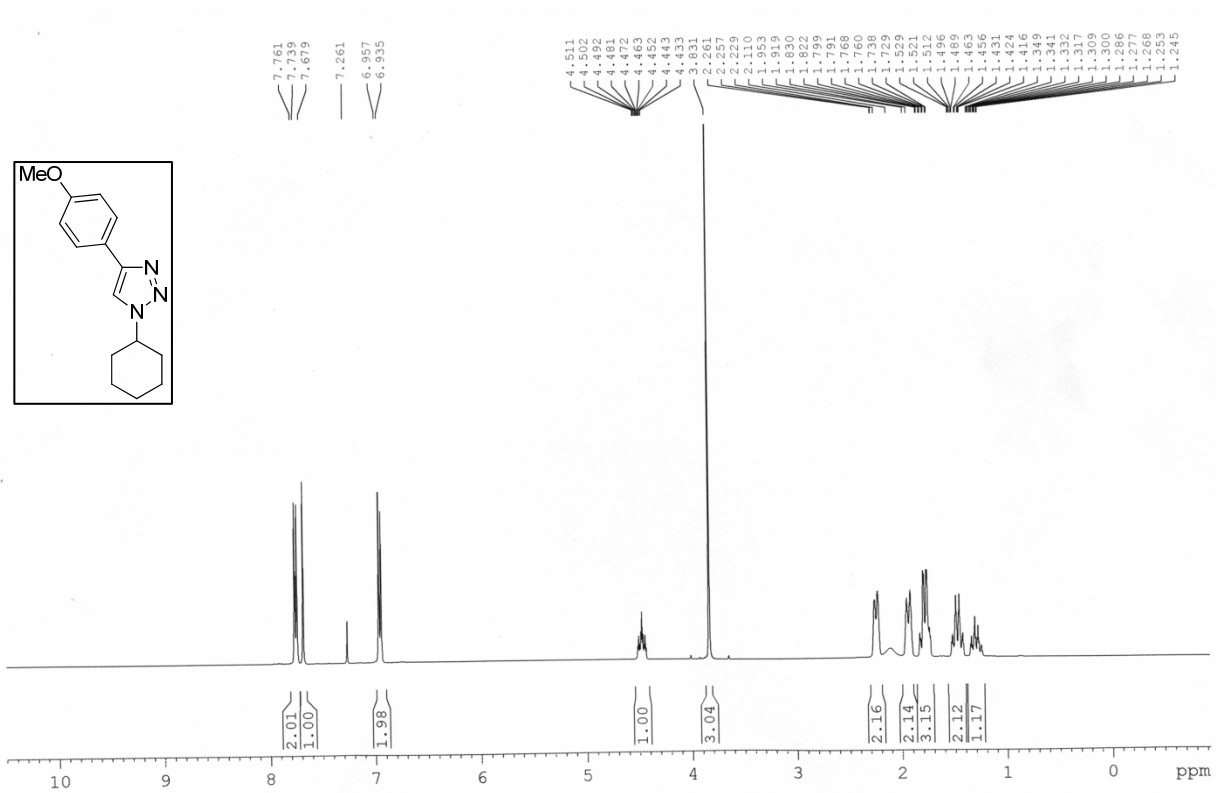


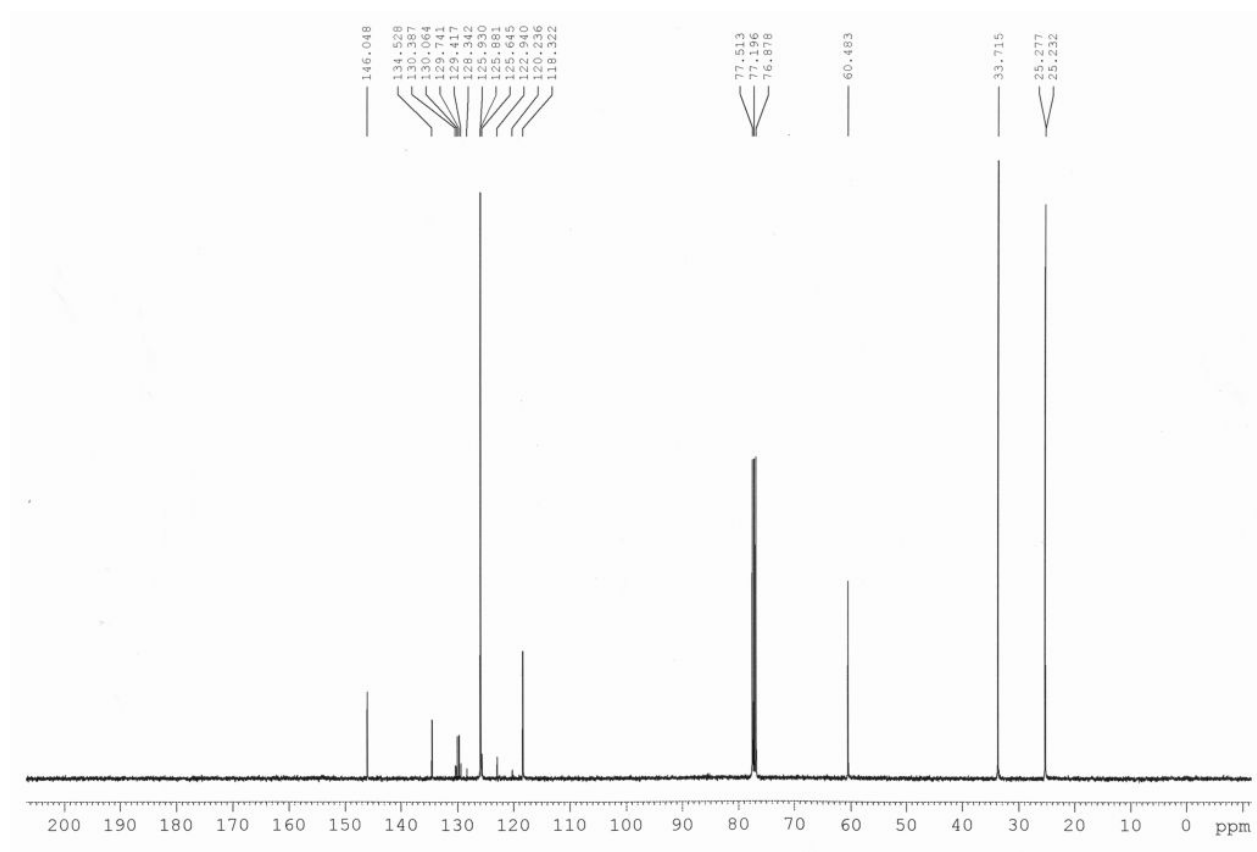
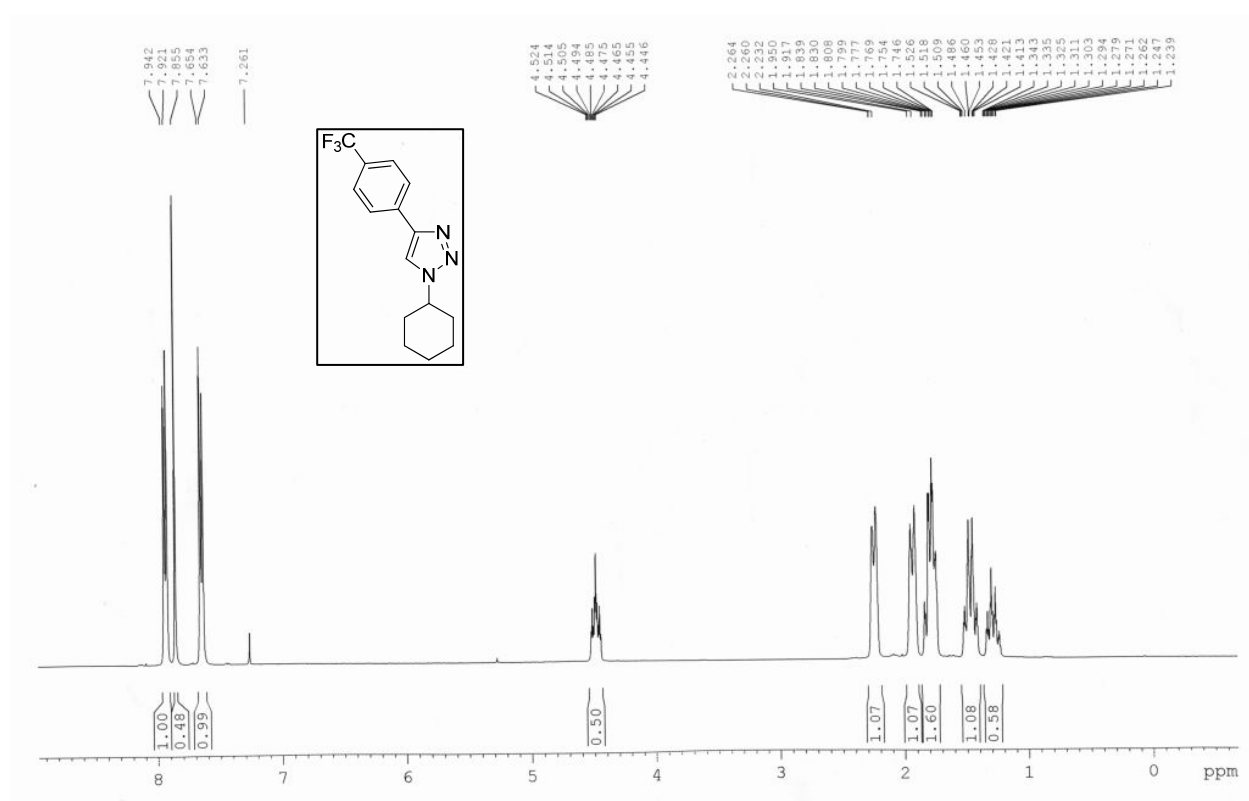




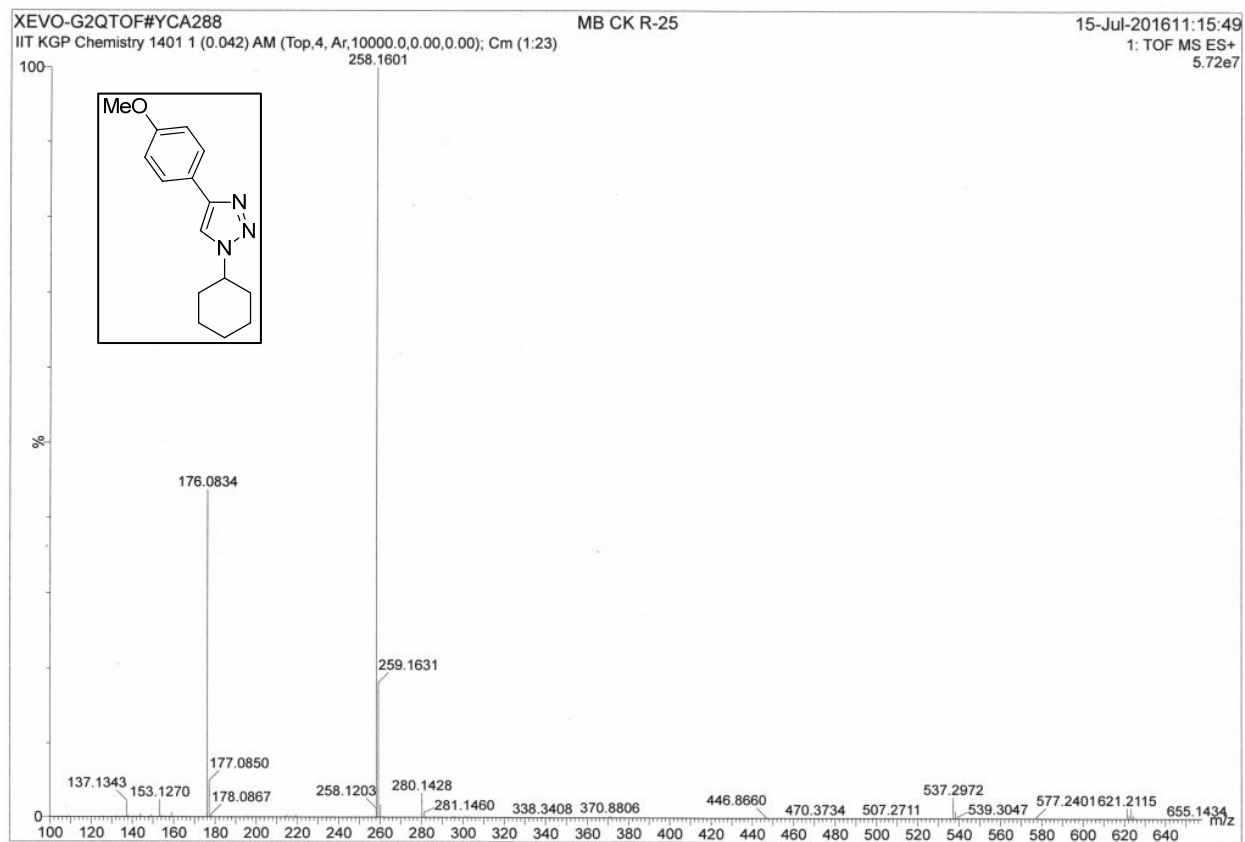








HRMS Spectra



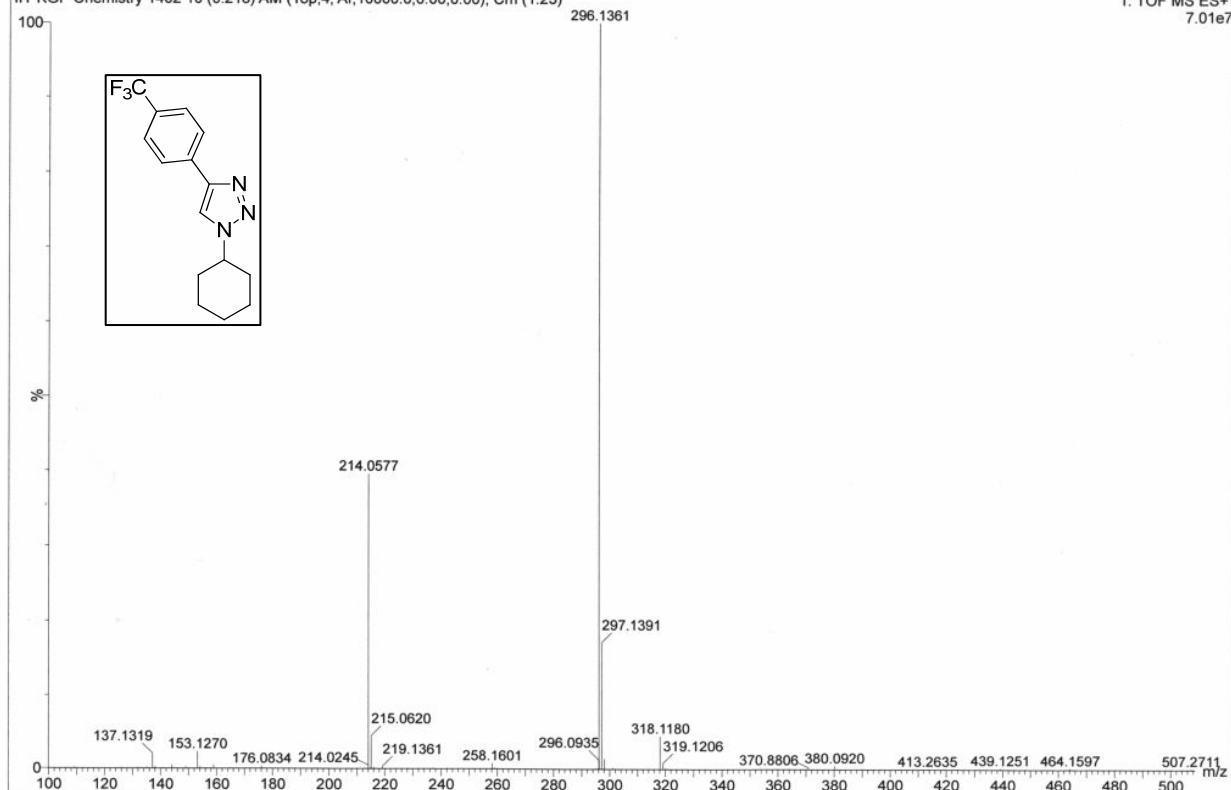
XEVO-G2QTOF#YCA288

MB CK R-32

15-Jul-2016 11:25:14

IIT KGP Chemistry 1402 10 (0.218) AM (Top, 4, Ar, 10000.0, 0.00, 0.00); Cm (1:23)

1: TOF MS ES+
7.01e7



NMR Spectra (^1H) (Products for cycloaddition of CO_2 to epoxides)

Yield Calculation of Cyclic Carbonates from ^1H -NMR

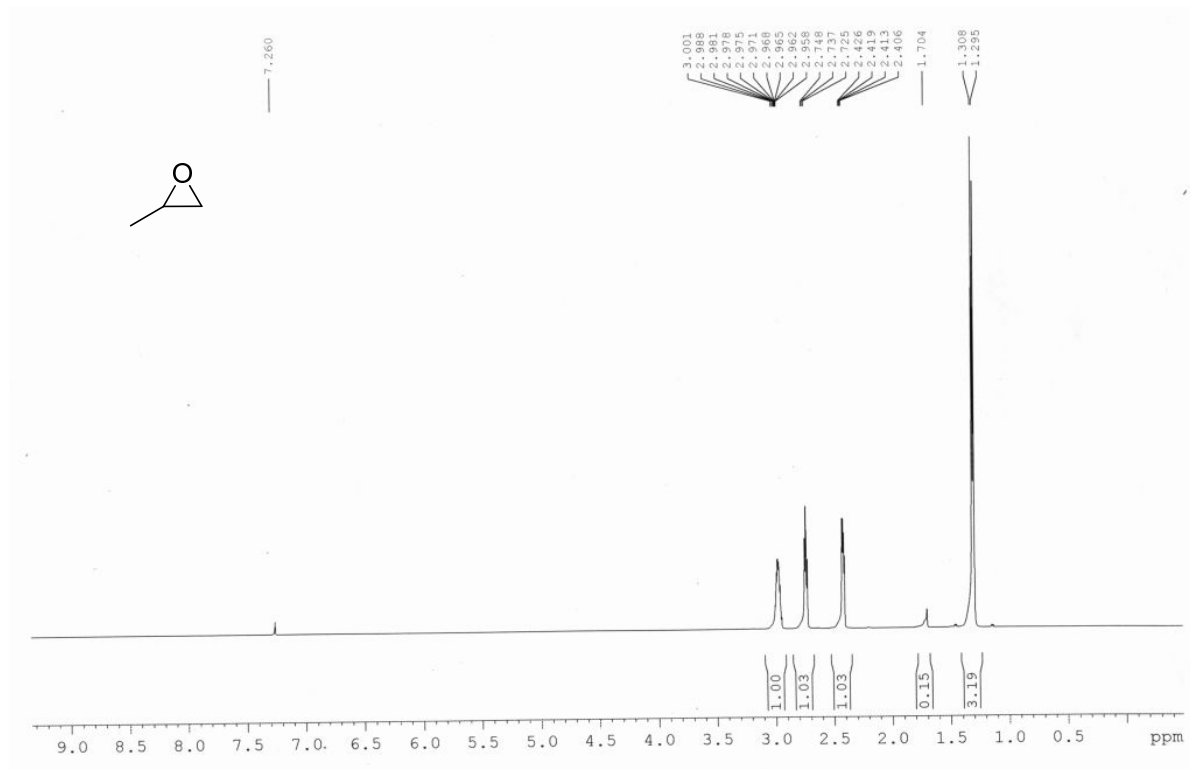


Figure S11. ^1H NMR spectra of propylene oxide (400 MHz, CDCl_3): $\delta = 3.00$ - 2.95 (m, 1H, O-CH), 2.74 (t, $J=4.4$ Hz, 1H, O- CH_2), 2.42 (q, $J = 2.8$ Hz, 1H, O- CH_2), 1.30 (d, $J = 5.2$ Hz, 3H, CH_3).

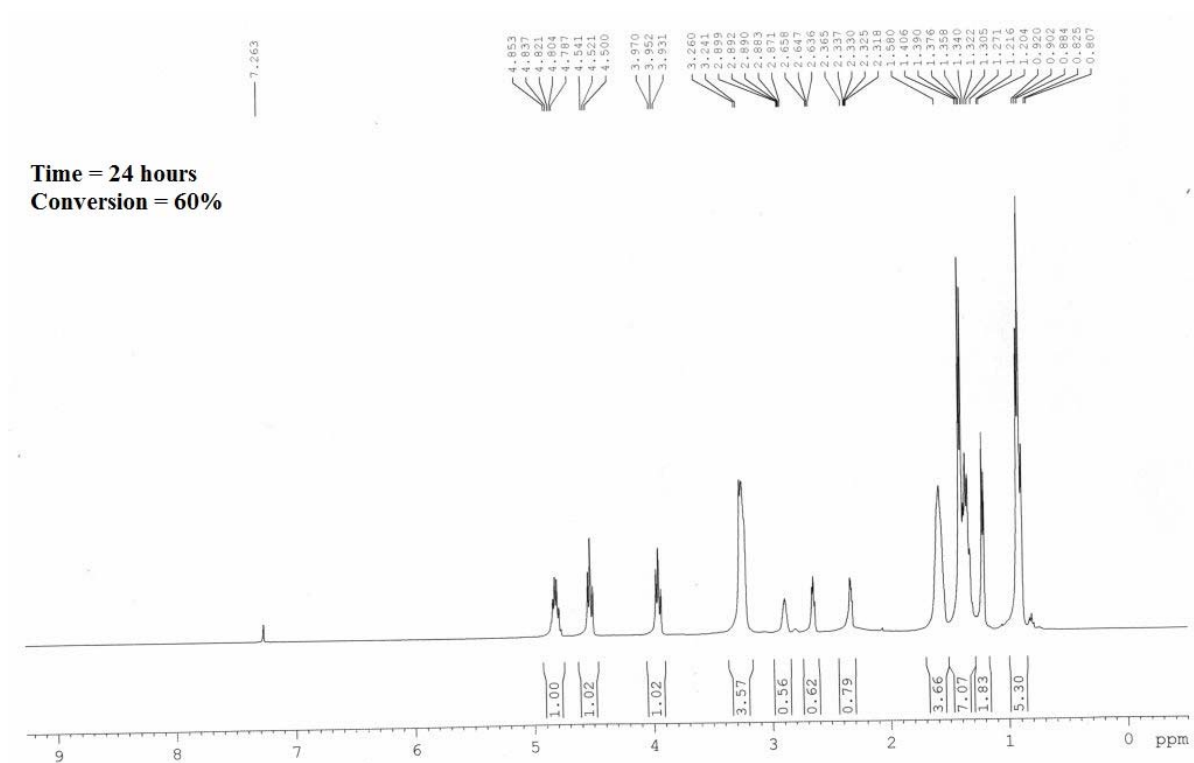


Figure S12. ^1H NMR spectra of the cycloaddition product of propylene oxide and CO_2 for 24h (400 MHz, CDCl_3) : δ = 4.85 – 4.78 (m, 1H, COO-CH), 4.54(t, J = 8.0 Hz, 1H, COO-CH₂), 3.97 (t, J = 8.4 Hz, 1H,COO-CH₂), 2.89 – 2.87 (m, 0.56H, O-CH), 2.65 (t, J = 4.4 Hz, 0.62H, O-CH₂), 2.33 (q, J = 2.8 Hz, 0.79H, OCH₂), 1.39 (d, J = 5.6 Hz, 4H, CH₃).

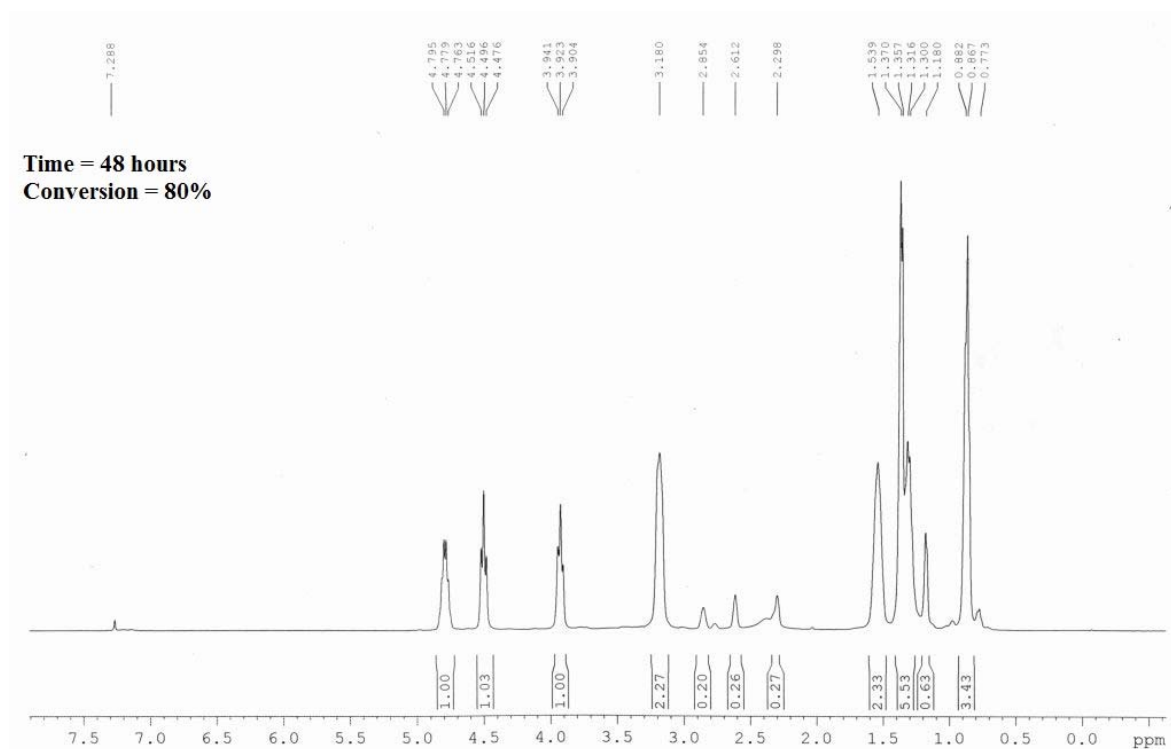


Figure S13. ¹H NMR spectra of the cycloaddition product of propylene oxide and CO₂ for 48h (400 MHz, CDCl₃) : δ = 4.79 – 4.76 (m, 1H, COO-CH), 4.51(t, J = 8.0 Hz, 1H, COO-CH₂), 3.94 (t, J = 7.6 Hz, 1H, COO-CH₂), 2.85 (b, 0.2H, O-CH), 2.61 (b, 0.26H, O-CH₂), 2.29 (b, 0.27H, O-CH₂), 1.37 (d, J = 5.2 Hz, 3.5H, O-CH₂).

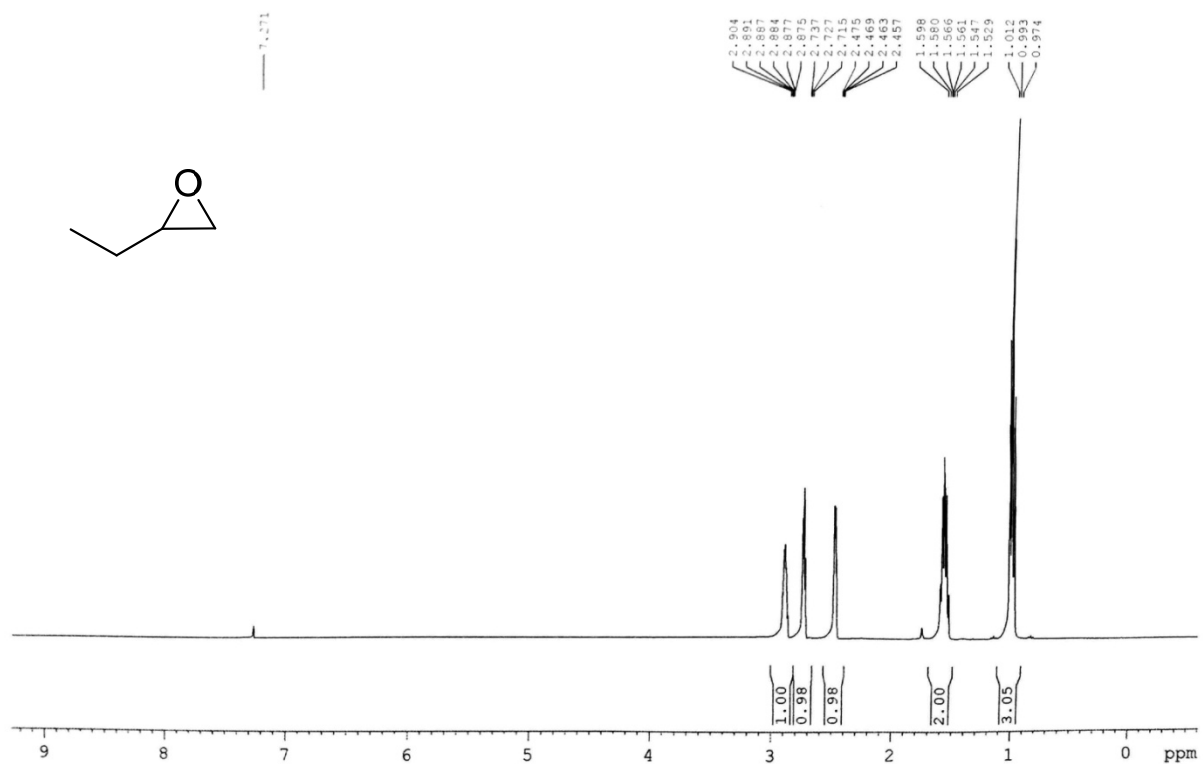


Figure S14. ¹H NMR spectra of 1,2-epoxy butane (400 MHz, CDCl₃): δ = 2.90 – 2.87 (m, 1H, O-CH), 2.73 – 2.71 (t, J = 4.4 Hz, 1H, O-CH₂), 2.47 – 2.45 (q, J = 2.4 Hz, 1H, O-CH₂), 1.59 – 1.52 (m, 2H, CH₂), 1.01 (t, J = 7.6 Hz, 3H, CH₃).

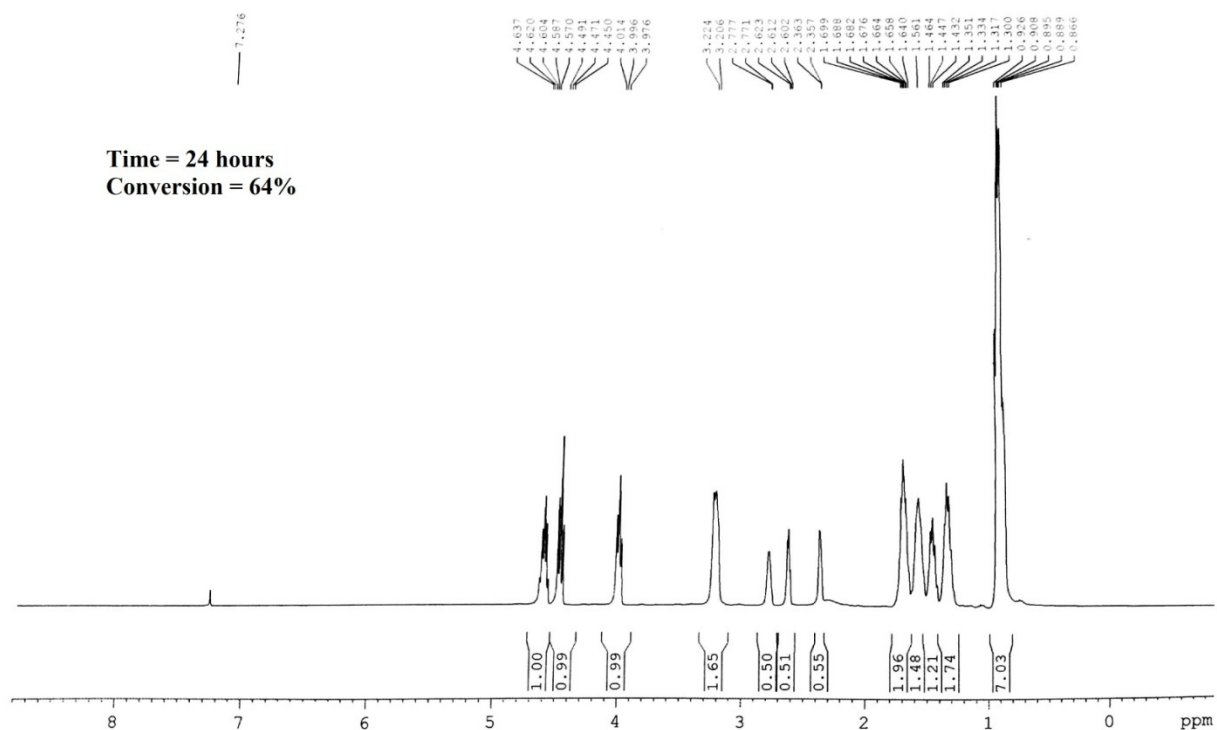


Figure S15. ^1H NMR spectra of the cycloaddition product of 1,2-epoxy butane and CO_2 for 24h (400 MHz, CDCl_3) : δ = 4.63 – 4.57 (m, 1H, COO-CH), 4.49 – 4.45 (m, 1H, COO-CH₂), 4.01 – 3.97 (m, 1H, COO-CH₂), 2.77 (m, 0.5H, O-CH), 2.62 – 2.60 (t, J = 4.4 Hz, 0.5H, O-CH₂), 2.36 – 2.35 (q, J = 2.4 Hz, 0.5H, O-CH₂), 1.69 – 1.64 (m, 2H, CH₂), 1.46 – 1.43 (m, 1H, CH₂), 0.92 (t, J = 7.2 Hz, 4.5H, CH₃).

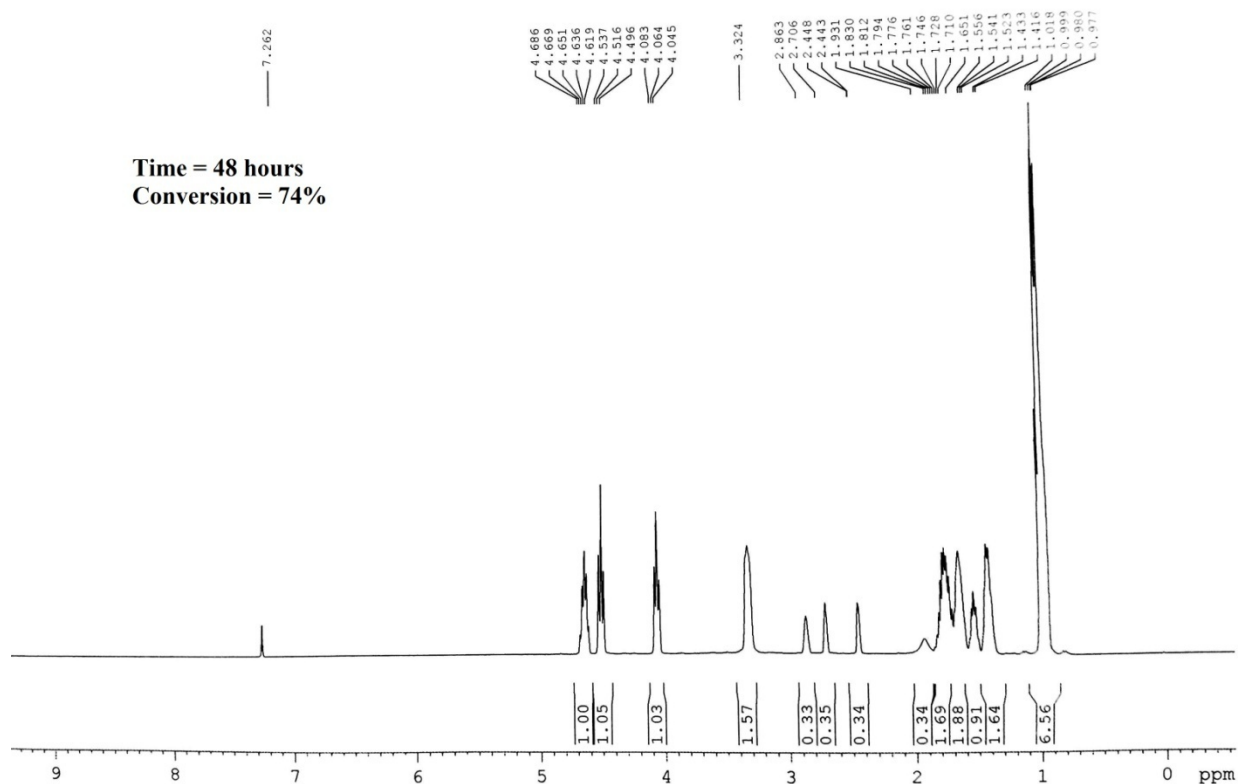


Figure S16. ^1H NMR spectra of the cycloaddition product of 1,2-epoxy butane and CO_2 for 48h (400 MHz, CDCl_3) : δ = 4.68 – 4.62 (m, 1H, COO-CH), 4.53 – 4.49 (m, 1H, COO-CH₂), 4.08 – 4.04 (m, 1H, COO-CH₂), 2.86 (m, 0.33H, O-CH), 2.70 (t, 0.35H, O-CH₂), 2.44 (q, J = 2.0 Hz, 0.34H, O-CH₂), 1.83 – 1.71 (m, 2H, CH₂), 1.55 – 1.52 (m, 0.9H, CH₂), 0.92 (t, J = 7.6 Hz, 4H, CH₃).

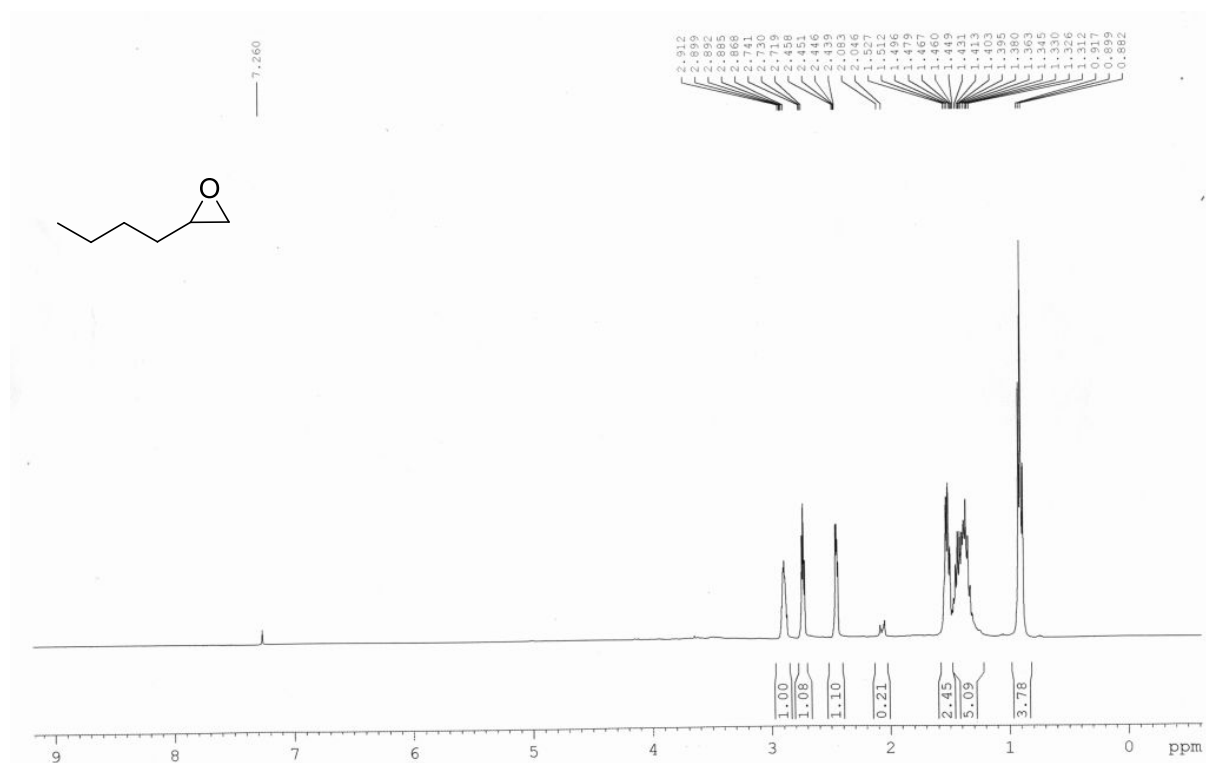


Figure S17. ¹H NMR spectra of 1,2-epoxy hexane (400 MHz, CDCl₃): δ = 2.91 – 2.86 (m, 1H, O-CH), 2.74 (t, J = 4.4 Hz, 1H, O-CH₂), 2.45 (q, J = 2.8 Hz, 1H, O-CH₂), 1.52 – 1.44 (m, 2H, CH₂), 1.43 – 1.31 (m, 4H, CH₂), 0.91 (t, J = 7.2 Hz, 3H, CH₃).

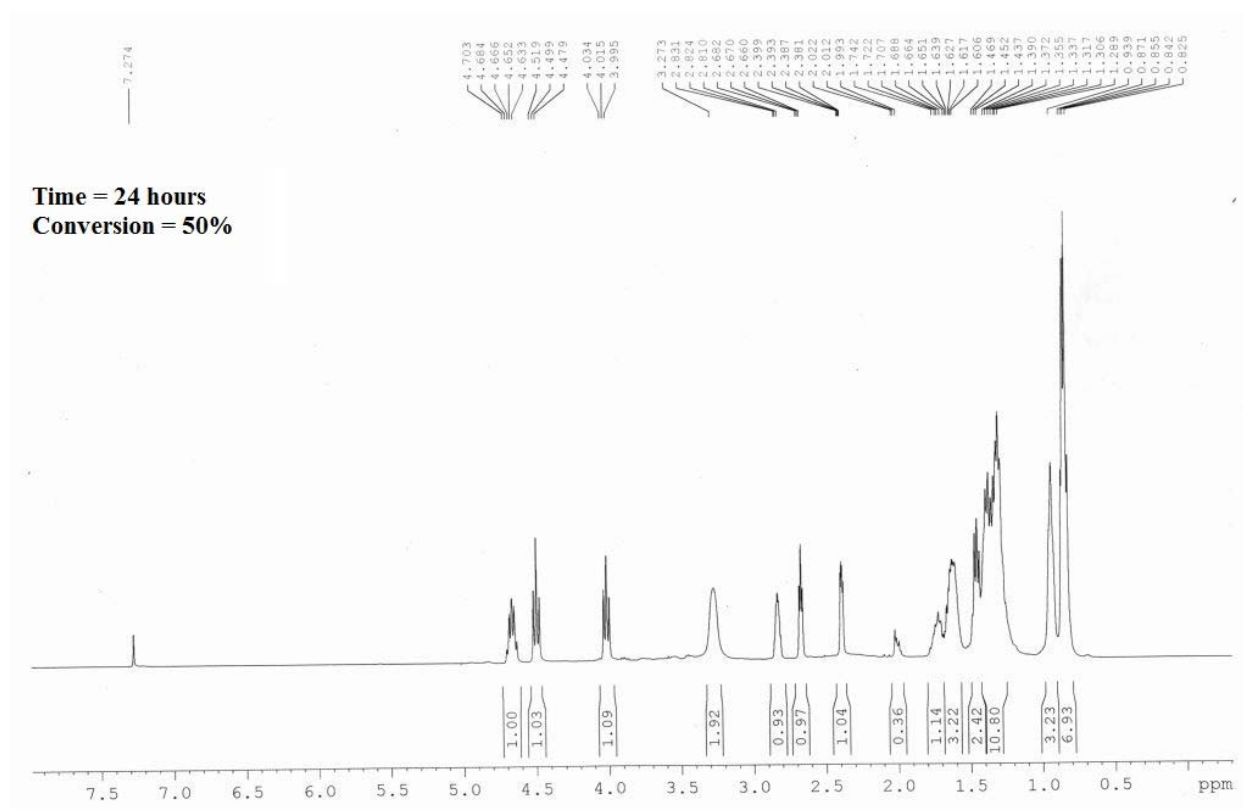


Figure S18. ^1H NMR spectra of the cycloaddition product of 1,2-epoxy hexane and CO_2 for 24h (400 MHz, CDCl_3) : δ = 4.70 – 4.63 (m, 1H, COO-CH), 4.51 (t, J = 8.0 Hz, 1H, COO- CH_2), 4.03 (t, J = 8.0 Hz, 1H, COO- CH_2), 2.83 (m, 0.93H, O-CH), 2.68 (t, J = 4.0 Hz, 0.97H, O- CH_2), 2.39 (q, J = 2.4 Hz, 1.04H, O- CH_2), 1.74 – 1.60 (m, 6H, CH_2), 1.46 – 1.28 (m, 6H, CH_2), 0.93 (b, 3H, CH_3), 0.87 (t, J = 6.4 Hz, 3H, CH_3).

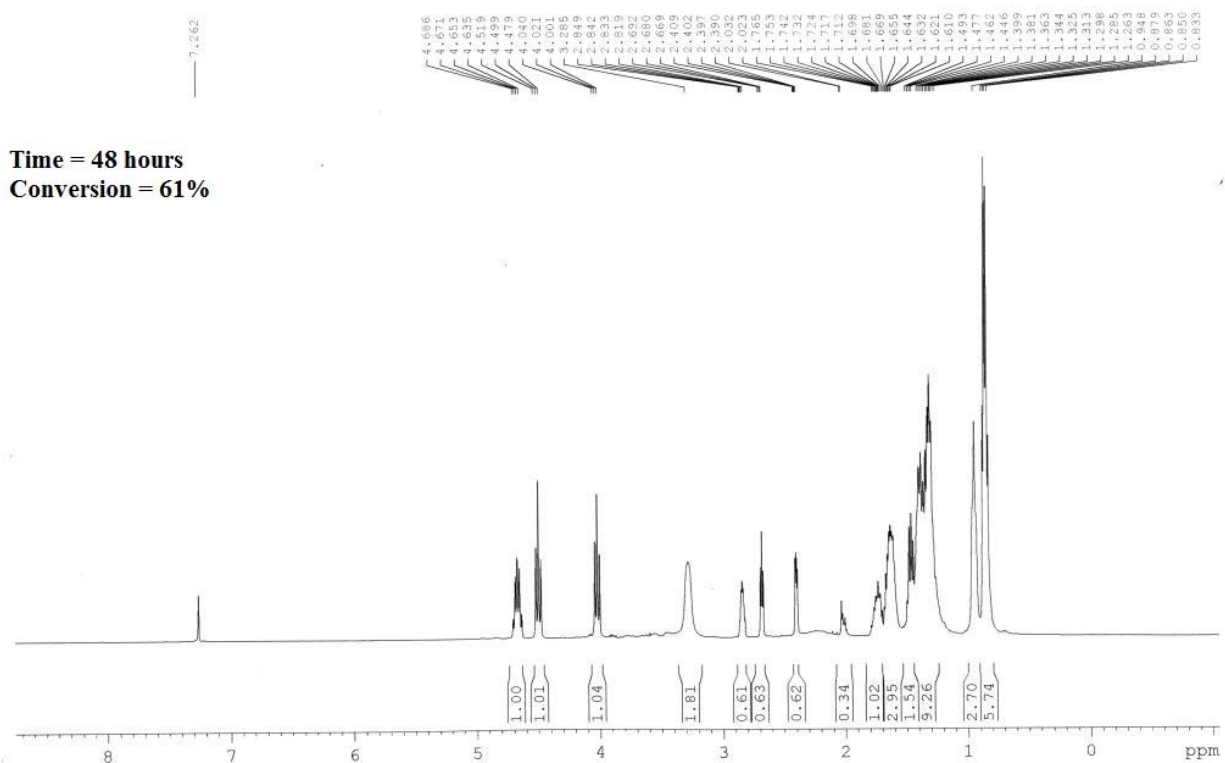


Figure S19. ^1H NMR spectra of the cycloaddition product of 1,2-epoxy hexane and CO_2 for 24h (400 MHz, CDCl_3) : δ = 4.68 – 4.63 (m, 1H, COO-CH), 4.51 (t, J = 8.0 Hz, 1H, COO- CH_2), 4.04 (t, J = 8.0 Hz, 1H, COO- CH_2), 2.84 – 2.81 (m, 0.61H, O-CH), 2.69 (t, J = 4.4 Hz, 0.63H, O- CH_2), 2.40 (q, J = 2.8 Hz, 0.62H, O- CH_2), 1.76 – 1.61 (m, 3.6H, CH_2), 1.49 – 1.26 (m, 6H, CH_2), 0.94 (b, 1.8H, CH_3), 0.87 (t, J = 6.4 Hz, 3H, CH_3).

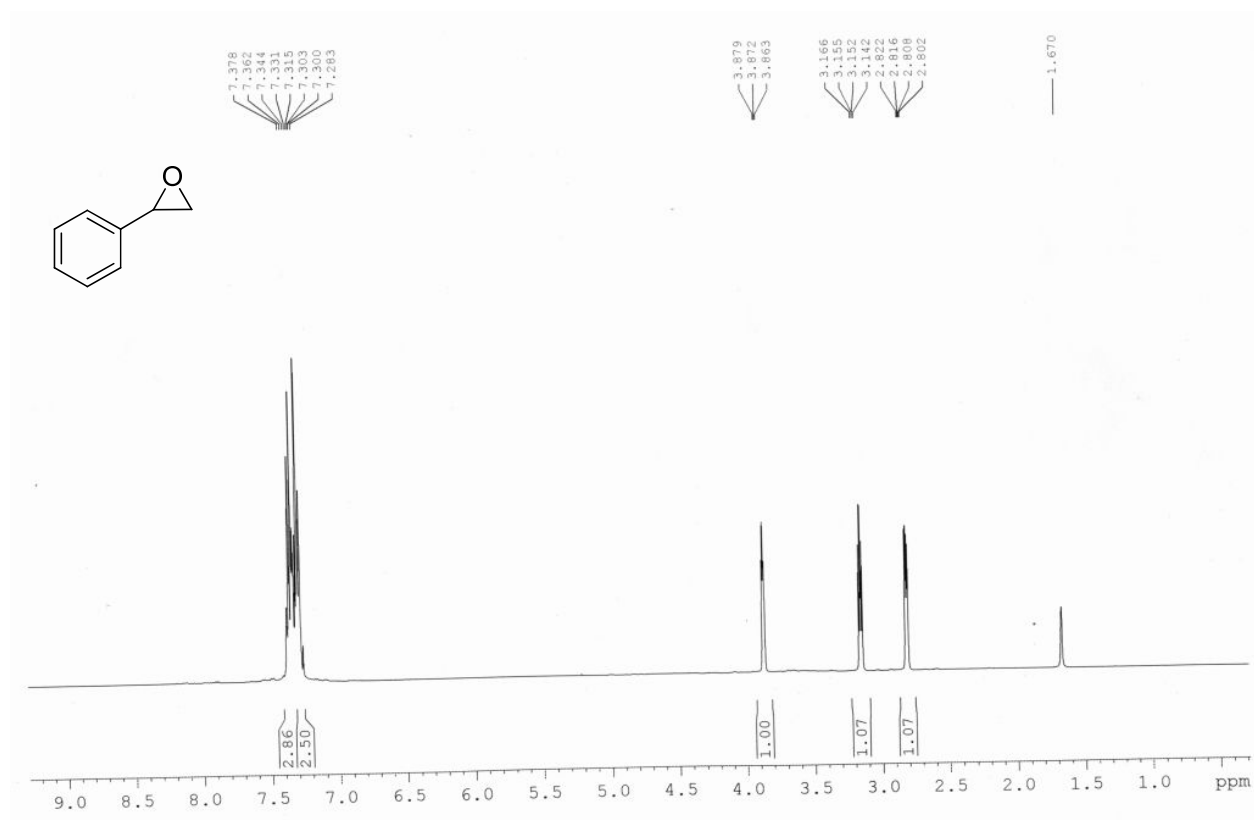


Figure S20. ¹H NMR spectra of styrene oxide (400 MHz, CDCl₃): δ = 7.37 – 7.28 (m, 5H, Ar-H), 3.87 (t, J =3.6 Hz, 1H, O-CH), 3.16 (q, J =4.0 Hz, 1H, O-CH₂), 2.82 (q, J = 2.4 Hz, 1H, O-CH₂).

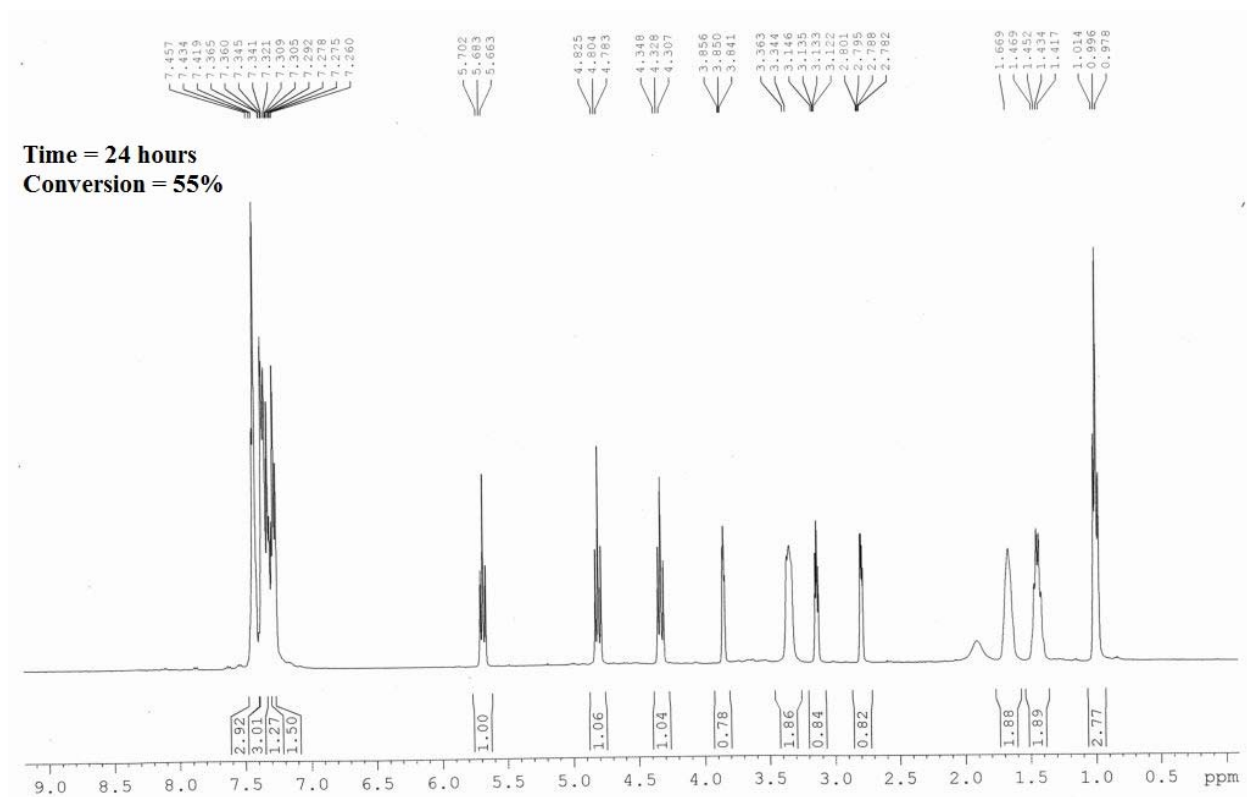


Figure S21. ^1H NMR spectra of the cycloaddition product of styrene oxide and CO_2 for 24h (400 MHz, CDCl_3) : δ = 7.45 – 7.26 (m, 9H, Ar-H), 5.70 (t, J = 8.0 Hz, 1H, COO-CH), 4.82 (t, J = 8.4 Hz, 1H, COO-CH₂), 4.34 (t, J = 8.0 Hz, 1H, COO-CH₂), 3.85 (t, J = 3.6 Hz, 0.78H, O-CH), 3.14 (q, J = 4.4 Hz, 0.84H, O-CH₂), 2.80 (q, J = 2.4 Hz, 0.82H, O-CH₂).

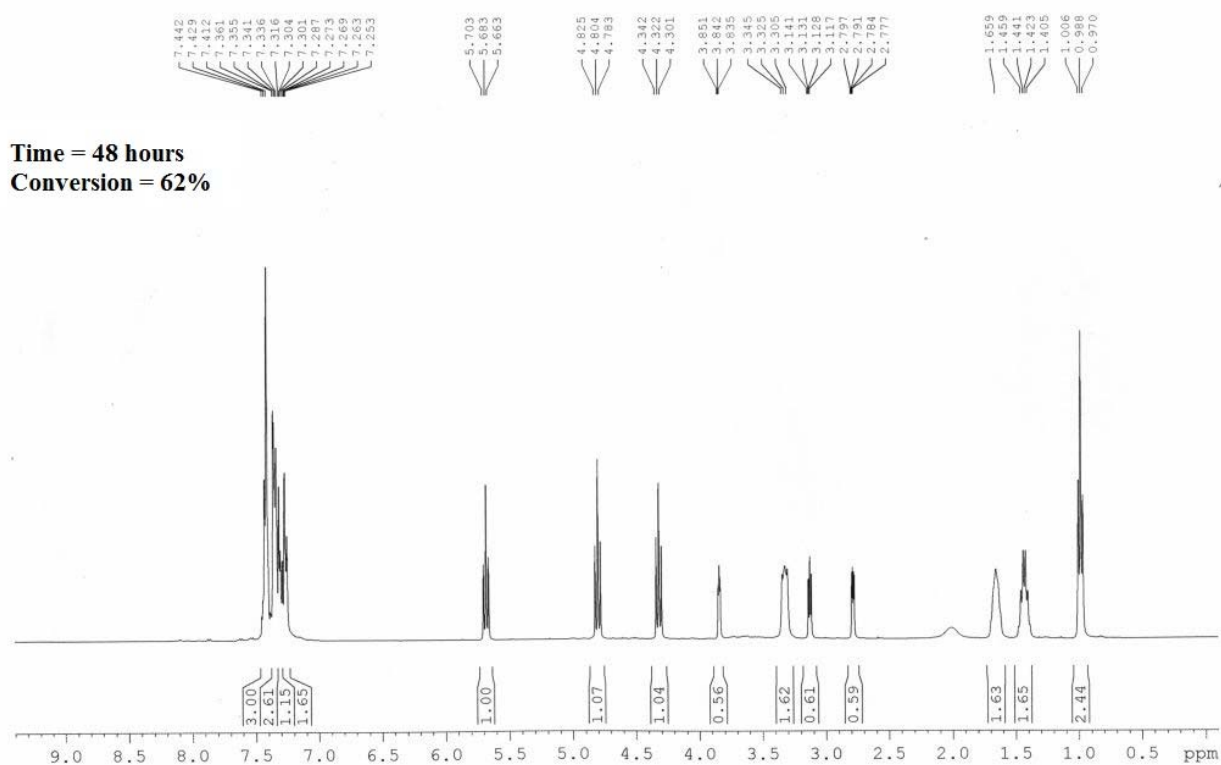


Figure S22. ^1H NMR spectra of the cycloaddition product of styrene oxide and CO_2 for 48h (400 MHz, CDCl_3) : $\delta = 7.44 - 7.25$ (m, 8H, Ar-H), 5.70 (t, $J = 8.0$ Hz, 1H, COO-CH), 4.82 (t, $J = 8.4$ Hz, 1H, COO- CH_2), 4.34 (t, $J = 8.0$ Hz, 1H, COO- CH_2), 3.85 (t, $J = 3.6$ Hz, 0.56H, O-CH), 3.14 (q, $J = 4.0$ Hz, 0.61H, O- CH_2), 2.79 (q, $J = 2.4$ Hz, 0.59H, O- CH_2).

References

1. Y. He, Z. Bian, C. Kang, Y. Cheng, L. Gao, *Chem. Commun.*, 2010, 3532–3534.
2. W. Jiang, J. Yang, Y.-Y. Liu and J.-F. Ma, *Chem. Commun.*, 2016, **52**, 1373–1376.
3. S. Sengupta and R. Mondal, *RSC Adv.*, 2016, **6**, 14009–14015.
4. A. Mallick, E.-M. Schon, T. Panda, K. Sreenivas, D. D. Diaz, R. Banerjee, *J. Mater. Chem.*, 2012, **22**, 14951–14963.
5. H. Li, Y. Zhu, J. Zhang, Z. Chi, L. Chen and C.-Y. Su, *RSC Adv.*, 2013, **3**, 16340–16344.
6. S. Sengupta, A. Goswami and R. Mondal, *New J. Chem.*, 2014, **38**, 2470–2479.
7. S. Samai and K. Biradha, *Chem. Mater.*, 2012, **24**, 1165–1173.
8. K. Asano and S. Matsubara, *Org. Lett.*, 2010, **12**, 4988–4991.
9. B. Wang, J. Zhang, X. Wang, N. Liu, W. Chen and Y. Hu, *J. Org. Chem.*, 2013, **78**, 10519–10523.
10. H.-W. Bai, Z.-J. Cai, S.-Y. Wang and S.-J. Ji, *Org. Lett.*, 2015, **17**, 2898–2901.
11. T. Kim, J. H. Song, K. H. Jeong, S. Lee and J. Ham, *Eur. J. Org. Chem.*, 2013, 3992–3996.